EVALUATING THE PRESERVATION OF HURRICANE DEPOSITS IN FLORIDA COASTAL SEDIMENTS

By

MARYLEA HART

A THESIS PRESENTED TO THE GRADUATE SCHOOL
OF THE UNIVERSITY OF FLORIDA IN PARTIAL FULFILLMENT
OF THE REQUIREMENTS FOR THE DEGREE OF
MASTER OF SCIENCE

UNIVERSITY OF FLORIDA

2003

This thesis s dedicated to my grandmother (Mimi) who has provided support and encouragement to three generations of my family while studying for their advanced degrees. Her educational values inspired me to continue my education beyond my bachelor's degree.

ACKNOWLEDGMENTS

I wish to thank my advisor, Dr. John Jaeger, for his patience and guidance throughout my thesis work. I would also like to thank my committee members, Dr. Mark Brenner and Dr. Paul Ciesielski, for their countless advice; and Dr. Jason Curtis for his assistance with lab work. Also, I wish to thank William Kenney for his lab assistance and for always having time to answer my endless questions. I also thank Lisa Marie Mertz for her help with lab work; and Donald Hardison and Jango Bhadha for hours of discussion and advice.

TABLE OF CONTENTS

page

LIST OF TABLES

LIST OF FIGURES

Abstract of Thesis Presented to the Graduate School
of the University of Florida in Partial Fulfillment of the
Requirements for the Degree of Master of Science

EVALUATING THE PRESERVATION OF HURRICANE DEPOSITS IN FLORIDA COASTAL SEDIMENTS

By

Marylea Hart

December 2003

Chair: John M. Jaeger
Department: Geological Sciences

Cyclones are one of the most energetic geomorphic agents in coastal environments of tropical, subtropical, and temperate latitudes, causing rapid changes in sediment deposition and erosion through intense wind and wave energy and coastal flooding. Since historical records of cyclone activity in the Atlantic Basin only extend back 370 years, a longer record is needed of past cyclone occurrences in order to better evaluate recurrence intervals (e.g., paleoclimate) and associated geomorphic change caused by cyclones. Coastal ponds offer an ideal location to study paleocyclone records because they offer an environment that is near the shoreline, that experiences little disturbance from waves and tides, and that has the potential for rapid sedimentation rates. Sand beds in muddy coastal ponds and marshes have frequently been associated with cyclone overwash deposition, although other transport agents (such as Aeolian) can result in similar type deposits. The purpose of this study was to evaluate a number of coastal pond sedimentary proxy records for their utility as paleocyclone indicators. Two sets of piston

cores were taken ~30 m from the beach in coastal ponds on St. Vincent Island, Florida, a relatively undisturbed island off the panhandle that has been frequently disturbed by hurricane activity. A variety of different proxy records (grain size, magnetic susceptibility, gamma bulk density, sediment reflectance, micropaleontology, salinity, %C and %N) were analyzed in these cores to detect three major hurricanes known to have severely impacted the island (in 1894, 1974-1975, and 1985), as well as additional minor hurricanes. Measurements of bulk density and magnetic susceptibility were obtained with a multi-sensor core logger, and cores were split and examined visually and x-radiographically for lithology. The cores were sampled at 1 cm intervals for measurements of radioisotopes (^{210}Pb, ^{226}Ra, and ^{137}Cs) and the aforementioned proxy records. Although it was difficult to establish a geochronology for Flag Pond due to the dynamics of sedimentary processes, results indicate an average sedimentation rate of 1.8-3 mm/yr. The sediment accumulation rate for Oyster Pond was calculated as 1.8 mm/yr based on ^{210}Pb activity. Grain size sorting of the sand fraction, percent sand, x-radiograph pixel density, and gamma bulk density data display some evidence of hurricane deposits corresponding to 1894, 1974-1975, and 1985; but the limitations of establishing a robust age-depth correlation prevent certainties in the correlation of the event layers to known hurricanes. Aeolian transport of sand makes it difficult to decipher extreme storms from less extreme storms. Modeling of the preservation potential of the these ponds indicates that a minimum storm bed thickness of one centimeter is needed in order for some portion of the bed to remain intact after passing through the surface-mixed layer. Dissipation time (the time required to completely destroy an event layer) for Oyster and Flag ponds is estimated to be ~5-10 years.

CHAPTER 1
INTRODUCTION

Tropical cyclones are one of nature's most destructive forces. The waves, winds, and rainfall associated with these storms can cause injury to humans, damage to property, flooding, and extensive landscape modification. With population increasing in coastal areas (Pielke and Landsea 1998) where cyclone strikes are most damaging, it would be helpful to insurance companies and landowners in coastal areas to have a record of the recurrence intervals of cyclones and the regions most likely to be affected by them in order to mitigate damage.

To understand the periodicity and intensity of cyclone activity for a region, a record of cyclone landfalls is needed that spans several thousands of years (Donnelly et al. 2001a). Although written historical accounts of tropical cyclone conditions from North America extend back 370 years, records of cyclone tracks maintained by the National Oceanic and Atmospheric Administration only extend back to the late nineteenth century. To extend this historical record, paleocyclone studies have been initiated that may provide important scientific information in two respects: (1) the frequency of cyclone strikes in a region can be calculated based on past occurrences of landfall; and (2) changes in cyclone patterns (e.g., intensity and frequency) in a region may provide information about the paleoclimate of that region.

A valuable method for studying paleocyclone activity is to examine the sediment record of coastal environments in tropical, subtropical, and temperate latitudes. The chemistry, mineralogy, and stratigraphy of sediments reflect depositional processes

associated with coastal agents, including cyclone activity. Abrupt changes in stratal composition may indicate an episodic erosional/depositional event associated with the impact of a cyclone. Coastal sedimentary strata have the potential to preserve a high-temperal resolution (decadal) record of cyclone activity if the particular depositional environment experiences high sedimentation and low biologic mixing rates.

Cyclone deposits in supratidal environments are typically the result of overwash deposition from storm surge flooding of an area. Hayes (1967) determined that storm surge is the dominant characteristic of cyclones, resulting in their importance as geomorphic agents. Cyclones also move sediment from offshore to onshore through wind and large waves. In past studies of cyclone deposition, several different proxy records of storm activity have been measured in cores from the continental shelf, salt marshes, coastal ponds, and coastal bays. Grain size and sorting are the most common proxies, but micropaleontology and organic C and N concentrations have also been used (Parsons 1998, Collins et al. 1999, and Donnely et al. 2001a). Cyclone beds are typically recognized as being more coarse-grained and poorly sorted than surrounding strata (Parsons 1998). In addition, during an intense storm, benthic marine foraminifera can be transported onshore from the continental shelf (Collinset al. 1999). In estuaries, coastal lakes, and salt marshes where the bottom sediments are fine-grained and organic-rich, lower organic C and N concentrations correlate with sand-rich layers that could be indicative of a storm deposit (Parsons 1998).

Recent studies indicate that it is necessary to study a combination of different proxy records to best identify paleocyclone deposition. Collins et al. (1999) report that using the presence of sand layers only to mark cyclones can underestimate the number of

storms. Since sand layers are usually only deposited near the location (within ~75 km) where the eyewall comes ashore, other parameters are needed to detect cyclone deposition. To complicate the matter, biologic and physical mixing can alter the appearance and preservation of distinct sand layers (Davis et al. 1989). For example, due to physical and biologic mixing, deposits left by Hurricane Andrew (Category 4) were only detectable through diatom assemblages in a Louisiana marsh 2 years after landfall, whereas initial deposits contained distinct sand beds (Parsons 1998). By increasing the number of proxy records that are used, storm layers can be better distinguished.

Although paleocyclone studies have been performed on a number of different coastal depositional environments (e.g., subtidal, intertidal, and supertidal) (Davis et al. 1989, Donnelly et al. 2001a, Liu and Fearn 2000), there is a lack of consensus as to which depositional environment consistently preserves the best record of cyclone activity. However, an ideal setting would fit the following criteria: (1) have high sedimentation rates to quickly bury event beds and prevent physical and chemical mixing; (2) experience regular cyclone activity resulting in likely production of paleocyclone indicators; and (3) are not influenced by frequent tidal fluctuations that may subsequently erode/mix event beds after deposition (Wheatcroft and Drake, 2002).

One environment that fits these criteria is a coastal pond. Coastal ponds are typically located very near the beach. Although subject to overwash deposits during cyclone activity, these ponds are separated from the beach environment by a sand barrier (e.g., barrier beach or dune ridge) and, thus, not regularly affected by tidal influences (Liu and Fearn 2000). Bottom sediments in coastal ponds are, in general, composed of mud-sized particles and organic matter (Liu and Fearn 2000). Sand and associated

marine microfossils from dunes, beaches, and offshore that are transported landward during a cyclone should be easy to differentiate from organic-rich material commonly found in these ponds. However, modern sea-level rise and associated landward migration of the surf zone over Holocene dune sediments and into ponds has the potential to influence the frequency of deposition of sandy, coarse-grained, poorly sorted intervals that may be interpreted as being cyclone deposits (Otvos 2002). Therefore, one must use caution when examining coarse-grained, poorly-sorted sediments in coastal ponds that date to times of sea-level rise, thus mistakenly interpreting these as cyclone deposits. Another complicating factor is that sand bed deposition in ponds often times is the result of extratropical storms (Otvos 2002). Although these storms are not characteristically as strong as cyclones, they do have the potential to deposit overwash and windblown material (Donnelly et al. 2001a). For example, Donnelly et al. (2001a) reported New England winter storms producing extreme storm surges similar in elevation but longer in duration than most cyclones. Also, vegetation, such as sea oats, is often located in the dune area between the ponds and the beachface, which could prevent the transfer of aeolian and overwash sediment by trapping and baffling flow. This would affect the type of deposit preserved in the sediment record.

Coastal ponds chosen for study of paloecyclone deposition also should be located in a region that is relatively undisturbed by human activity. Urban development often results in increased runoff of coarse-grained material from inland areas into low-lying ponds (Applelboom et al. 2002) could be misinterpreted as cyclone deposits. St. Vincent Island located along the western panhandle of Florida, offers an ideal environment for studying paleocyclone activity (Figure 1-1). The island is geographically located in an

area regularly impacted by cyclones (i.e., hurricanes), there are a number of fresh and saltwater ponds to study, and there has been minimal human disturbance.

The goal of this project was to examine the recent sedimentological record (past 100 years) of St. Vincent Island for evidence of historical hurricanes. Only recent sediments were studied because of the limitations of the chronological techniques (^{210}Pb) and historical data of cyclone activity with which to compare the deposits found in the sediment record. The data set used to address two scientific questions: which proxy records are best used to identify hurricane deposits along the northern Gulf of Mexico coastline, and what sedimentary conditions in coastal ponds provide the best preservation potential?

The few studies done on recent (post 1968) hurricane deposits from coastal environments such as salt marshes, coastal ponds, and coastal bays (Risi 1998, Collins et al. 1999) suggest general characterizations that allow for the following basic hypotheses to be tested by this research:

- Because coastal ponds often contain fine-grained, organic mud-rich sediments, the coarse-grained, poorly-sorted sands typically associated with hurricane overwash should be easily distinguishable.
- Because of the higher sand content associated with cyclone deposits, bulk density should show similar increases.
- Particular species of foraminifera are specific to the marine environment. Their presence in coastal ponds could be indicative of overwash (Collins et al. 1999).
- Overwash deposits in muddy ponds could be observed by a decrease in organic carbon and nitrogen concentrations that correlates with increased accumulation of poorly sorted sand.
- Because of the presence of magnetic minerals in offshore sediments (Wheeler et al. 1999), increases in magnetic susceptibility could correlate with overwash.

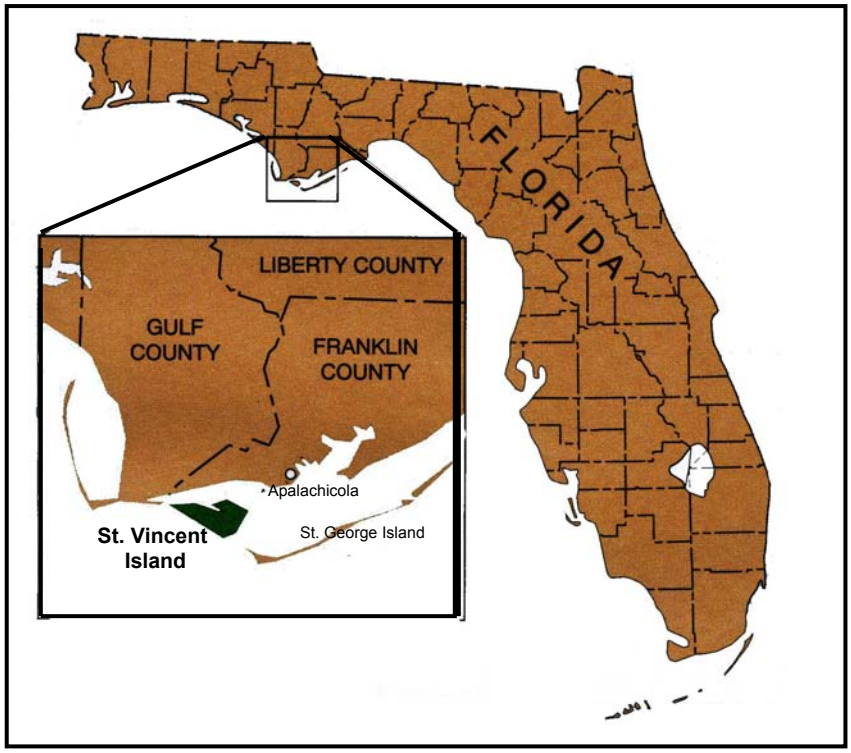

Figure 1-1. Location of St. Vincent Island drafted from a figure Davis, J.H. and Mokray, M.F. (2000) Assessment of the effect of road construction and other modifications on surface-water flow at St. Vincent National Wildlife Refuge, Franklin County, Florida. *USGS Water-Resources Investigations Report 00-4007.*

CHAPTER 2
BACKGROUND INFORMATION

Signal

The geologic record contains abundant strata that are associated with the occurrence of natural disasters (e.g., volcanic ash beds, river flood deposits). Some layers are well preserved and easily identified through visual examination. Other layers are more difficult to visually detect and require the use of biostratigraphic, petrologic, and geochemical markers (i.e. forams, diatoms, % C, % N) (Collins et al. 1999; Parsons 1998). Also, multiple depositional processes can produce the same signal in just one tracer. It is, therefore, necessary to study a number of different proxy records in order to clearly define geologic deposits generated by particular natural disasters.

Hurricanes can produce recognizable deposits in coastal regions due to flooding from intense precipitation or storm surges (Ball et at. 1967, Davis et al. 1989, Risi 1998, Liu and Fearn 2000). Hurricane stratal characteristics vary depending on storm intensity, landform shape, distance of sampling site relative to where the eyewall comes ashore, forward speed and duration of storm, amount of rainfall, and local sedimentary environment (i.e., subtidal, intertidal, supratidal) (Davis et al. 1989, Risi 1998). In addition, storm deposits can be altered within months through natural sediment mixing by physical and biological processes, yet still be detectable through biostratigraphic evidence (Parsons 1998 and Collins et al. 1999).

Davis et al. (1989) reported the deposition of hurricane beds in cores from two coastal bays along the west-central coast of Florida (Figure 2-1). Hurricanes are credited

as being a major contributor to the Holocene stratigraphy of Sarasota Bay and Little Sarasota Bay. Cores were analyzed for textural properties and macrofaunal content. Three types of storm facies were identified within the cores (Figure 2-2). The graded storm facies is characterized by the transport of shelly sediment into bays. This facies is the result of an intense storm, most likely a hurricane. The homogeneous facies represents the reworking of bay sediments during strong frontal passages or weak hurricanes. The fluvial storm facies is produced by runoff of terrigenous material into the bays as the result of extreme rainfall. Although there is some geographic control on the location of the different facies due to available parent material, they can generally be found in the same region within Sarasota Bay.

Liu and Fearn (1993 and 2000) studied seven cores from Lake Shelby and Middle Lake, Alabama and sixteen cores from Western Lake, Florida (Figure 2-3). Lake Shelby and Middle Lake are freshwater lakes that are separated from the Gulf of Mexico by 250 m of sandy, pine-dominated beach ridges and sand dunes that are 2-4 m high. A canal dug in 1960 connects the two lakes. A 150-200 m wide barrier beach separates Western Lake from the Gulf of Mexico. The lake maintains salinities between 2.5 and 5.5 ppt due to a restricted connection with the Gulf 1 km to the north of the lake. Sand layers were identified using visual observations and water and organic matter content. The cores taken from these lakes showed a noticeable absence of thick sand layers below ~3 m attributed to minimal cyclone activity prior to 3.2 ka (^{14}C). Liu and Fearn (1993 and 2000) suggest that the absence coincides with an abrupt regional climate change documented by Hodell et al. (1991) based on oxygen isotope data from a core from Lake Miragoane, Haiti. The isotope data indicates that there was a sudden onset of drier

conditions around this time that caused higher evaporation rates and lower lake levels in Haiti. Liu and Fearn suggest that there may have been a regional shift in circulation patterns that caused cyclones to change their paths to a more eastern track. Between 4.5 and 3.2 ka, the Pecos River Basin in SW Texas experienced severe flooding, followed by a period of infrequent flooding, suggesting a change in weather patterns (Patten and Dibble 1982). Based on their data, combined with the data from Haiti and SW Texas, Liu and Fearn believe that before 3.2 kya cyclones followed a western track when they entered the Gulf of Mexico and struck the coasts of Texas and Louisiana; but an abrupt change in circulation patterns occurred around 3.2 kya that caused cyclones to switch to a more easterly track, hitting Florida and Alabama more frequently. However, given late Holocene sea level rise (~1.6 mm/yr) (Bard et al. 1996), sea-level would have been 4-5 meters lower at this time than today. Given a nearshore slope of 1/60 (NOAA Bathymetric Charts), the shoreline would have been ~300 m further seaward. This increased distance may have contributed to the lack of sandy bedding prior to 3.2 kya.

Parsons (1997) examined cores from a salt marsh pond on the Louisiana coast to determine if a hurricane layer associated with Hurricane Andrew (1994) could be distinguished and, if so, the origin of sediments in the hurricane layer (Figure 2-4). Deposits were identified using grain size, sediment pigments, organic content, and diatom analysis. The results showed that the sediments were imported and reworked from a variety of environments and that the layer could be distinguished one year after deposition. Two years after deposition, the layer was only distinguishable through diatom assemblages. The only sedimentological evidence of Hurricane Hugo in fresh water ponds 50 to 75 km apart and parallel to the coast from the landfall location, was the

presence of marine forams at the depth corresponding to the time of Hugo's landfall (Collins 1999).

Donnelly et al. (2001a; 2001b) describe evidence of hurricane overwash deposits in cores from salt marshes in New Jersey and Rhode Island (Figure 2-5). The purpose of these studies was to reconstruct the overwash history of a back-barrier salt marsh in order to provide a landfall frequency of intense storms. Nine cores were taken in a grid 50 m apart from Whales Beach Marsh in New Jersey. The marsh is approximately 250 m from the shoreline. Fourteen cores were taken in the Succotash Marsh, Rhode Island along transects that went inland from the coast. Succotash Marsh is located 275 m from the shoreline. Deposits were identified visually for changes in lithology. The cores were dated with ^{14}C and ^{137}Cs. Pollen stratigraphy provided additional age control. Four of the six identified overwash deposits were matched to historical photographs from periods of known overwash. The remaining two overwash fans were dated to between 592 and 570 years B.P. and the other dated to roughly six hundred years B.P.

Preservation of Hurricane Deposits

There have been numerous studies done on storm bed deposition directly after a hurricane has impacted an area, but few studies have been completed on the preservation of these deposits through time (Ball et al. 1967, Perkins and Enos 1968, Davis et al. 1989, Liu and Fearn 2000). Storm intensity and deposit location within the coastal zone (e.g., intertidal, or supratidal) determine the preservation potential for a deposit (Davis et al. 1989). Supratidal sediments are likely to preserve a better record of cyclone overwash, as only powerful hurricanes (Category 4 or 5) can transfer material from offshore into the supratidal environment (Collins at al. 1999). Also, sediments deposited above the normal high tide mark are more likely to be preserved because this environment is not constantly

subject to wave resuspension and mixing. Collins et al. (1999) reported that subtidal deposits of hurricanes were not visually or geochemically decipherable three years after their deposition.

Wheatcroft and Drake (2002) report that there are four main factors controlling the preservation potential of sedimentary event beds in the marine environment: 1) sediment accumulation rate, 2) mixing layer thickness, 3) bioturbation intensity, and 4) event layer thickness. The sediment accumulation rate determines the time required for an event layer to be buried and, therefore, better preserved within the sediment record. Low sedimentation rates allow the event layer to be exposed to physical and biologic mixing for a greater amount of time allowing the preservation potential to be influenced by the other three factors to a greater degree (Ravichandran et al. 1995).

The surface mixed layer thickness refers to the depth below the sediment-water interface at which mixing typically occurs through physical or biological processes. Bioturbation, in the form of deposit feeding, burrowing, and tube building, can cause mixing of an event signal within sediments. Bioturbation is more intense at the sediment-water interface, where infaunal organisms are more numerous and decreases with depth. Mixing intensity can be measured by naturally occurring tracers (^{234}Th, ^{7}Be, and ^{210}Pb) and synthesized tracers (glass beads, luminophores, and radio-labeled particles). A deeper mixing layer (>5 cm) would greatly inhibit preservation of event layers. If an event layer is thicker than the surface mixed layer is deep, some will be preserved (Wheatcroft and Drake 2002). Shallower mixing layer depths coupled with high sediment accumulation rates would favor preservation of signal layers (Ravichandran et al. 1995). Environments with low accumulation rates, such as lakes and estuaries, are at

a greater risk of signal loss through bioturbation because the animals have an increased amount of time (5-10 years) to mix the event layer (Ruiz-Fernandez et al. 2001).

The preservation potential of an event layer is proportional to its original thickness and the speed at which it is advected through the surface mixed layer by burial (i.e. sedimentation rate). For example, in a marine environment Wheatcroft and Drake (in press) found a thin layer (<1 cm) would be difficult to preserve because other factors, such as bioturbation, would not require much time (months to years) to destroy the signal, unless in an area of high sedimentation (1-5 cm/yr) or low mixing (0-0.1 cm^2/yr). Thicker deposits would require more time and energy to be dispersed. Wheatcroft and Drake (in press) also found that an event such as a flood or hurricane, followed subsequently by another event, increases the sedimentation rate and allows for quick burial of the signal left by the first event.

Coastal Ponds

There is no clear definition of the geomorphology or depositional facies of coastal ponds and lakes. Those mentioned in available scientific literature are generally 0-15 km from the mean high water mark and vary in area and in depth (e.g. Liu and Fearn 1993 and 2000, Collins 1999, Norton et al. 1997, and O'Sullivan et al. 1991). Some ponds and lakes are tidally connected and are saline to brackish, while others remain fresh.

Sediment accumulation rate measurements in these ponds are sparse, but range from ~1 to 50 mm/yr, with the average being ~5 mm/yr (O'Sullivan et al. 1991, Norton et al. 1997, Scott and Steenkamp 1996, Ravichandran et al. 1995, Williams 1995, and Hyatt and Gilbert 2000). In comparison, the sediment accumulation rates for inland Florida lakes range from 0.2-2 mm/yr (Schelske et al. 2001). Very little research is available on the sediment mixing rates in coastal pond sediments. A study by Ravichandran et al.

(1995) estimated the mixing coefficient for Sabine Lake, located along the Texas coast, to be ~0.04-0.4 cm^2/yr based on measurements of $^{239,240}Pu$. Mixing rates for other coastal areas are higher and include 0.3-2.5 cm^2/yr for New York Bight, 4-32 cm^2/yr for Narragansett Bay, Rhode Island, and 0.1 to 100 cm^2/yr for lacustrine and marine environments in general (Santschi et al. 1980 and Boudreau, 1994).

Study Area

The Gulf Coast of the United States is regularly impacted by tropical storms and hurricanes. Due to prevailing wind currents, hurricanes over the past 200 years have moved north to northwest when entering the Gulf of Mexico (Williams and Duedell 1997). While it is uncommon for hurricanes to hit the west coast of the Florida peninsula, the panhandle is frequently affected by such storms. Fifty-six percent of the hurricanes to hit the Florida panhandle from 1885 to 1984 occurred in the Apalachicola Bay area (Davis et al. 1989) (Figure 2-6).

One region in the Apalachicola Bay area that has been severely impacted by hurricane landfall is St. Vincent Island, a Holocene barrier island located on the Gulf side of the Apalachicola Bay. The island regularly experiences hurricanes moving onshore from the Gulf of Mexico (National Hurricane Center) (Figure 2-7). The island was managed as a hunting preserve until 1908, when Dr. R. J. Pierce purchased the island for use as a hunting area. Over 125 kilometers of dirt roads were built throughout the island to allow access for timber companies to log the island in the 1940s and 1960s (Doyle and Krauss 1999). Three permanent structures were built on the island and a dock is located on the western tip. Some of the ponds were managed for freshwater fishing purposes. When the Wildlife Refuge took over in 1968, culverts, dams, and other water control structures were put into place. The ponds have been managed as both salt and freshwater

over the last 30 years. The Wildlife Refuge is currently attempting to return the ponds to their natural, brackish state. Vegetation in some areas of the island is maintained by fire, both prescribed and natural. Despite past development, the Wildlife Refuge considers the island to be in a natural condition (St. Vincent National Wildlife Refuge, Apalachicola, Fl., 2000, Wildlife and Habitat Management Review, May 31-June 2, 2000.).

St. Vincent Island is 15 km long by 7 km wide and covers ~50 km^2. The island is separated from the mainland by the Apalachicola Bay and the St. Vincent Sound. The elevation of St. Vincent ranges from 0 to ~4 meters above mean high water level. The island is primarily composed of quartz sand with the exception of muddy marshes, which contain sand-clay, silt, and organic-rich matter (St. Vincent National Wildlife Refuge, Apalachicola, Fl. ,1968, 1968 Narrative Report. US Department of the Interior, Fish and Wildlife Service, Bureau of Sport Fisheries and Wildlife, 23p.).

The morphology of the island is characterized by a system of twelve beach ridge sets, formed between 6000 to 800 years B.P., possibly through cyclicity in late Holocene sea level, that runs northwest to southeast, a large marsh, and approximately fourteen enclosed fresh and saltwater lakes (Campbell 1986) (Figure 2-4). Flag Pond is located on the south side of the island with its south shore approximately ~275 m from the island's south beach face. It has a surface area of approximately ~25 m^2 and a depth of ~0.5 to 1 m. Oyster Pond is located to the east of Flag Pond and is approximately ~400 m from the south beach. The pond has surface area of approximately ~350,000 m^2 and a depth of ~0.5 to 1.5 m (USGS 7 ½ Minute Quadrangle Map – Indian Pass, Fl.).

Known Hurricanes of St. Vincent Island Region

There have been 60 tropical cyclones to follow a course within a 150 km radius of St. Vincent Island in the last 100 years. Of these, 19 were hurricanes with winds greater

than 110 km/hr and two hurricanes had winds greater than 160 km/ St. Vincent National Wildlife Refuge, Apalachicola, Fl., 2000, Final Report of the Vegetation Survey and Map Project, A USFWS-USGS Research Partnership Program Project.) (Table 2-1). Documentation of damage done by hurricanes and other major storms to hit St. Vincent Island does not begin until the Wildlife Refuge took over the island in 1968. The refuge puts out an annual report that documents any major weather events that happen during the year, and all of the accounts in this section are from those reports unless otherwise indicated. However, these reports only contain information on specific damage to the island and it is assumed that other forces, such as wind, rain, and high tides, also affected the island during these storms.

Williams and Duedell (1997) report six hurricanes in the vicinity of St. Vincent Island in the years 1885 (2), 1886 (2), 1894, and 1898. One of the 1886 hurricanes crossed directly over the island and was classified as a Great Hurricane (Category 5). A tree ring study performed on St. Vincent Island by Doyle and Krauss (1999) showed evidence of the 1894 hurricane, which had wind speeds sufficient to thin forests on the island, as indicated by suppressed and released growth patterns, as hurricanes cause crown and root damage on the windward side of trees resulting in less radial growth. Williams and Duedell (1997) report another hurricane struck Carrabelle, FL. (~45 km northeast of St. Vincent Island) on August 1, 1899. The storm remained in a stationary position for 10 hours, leaving the town severely damaged.

The first hurricane documented in the Wildlife Refuge reports, Hurricane Agnes, occurred on June 18 and 19, 1972. Although wind gusts in Carabelle would not even qualify this storm as Category 1 on the Saffir-Simpson Hurricane Scale, storm surges of

~2 meters above astronomical predictions qualify it in this category. The magnitude of the storm surge put this storm in the 50-year storm category (Table 2-2). The 1972 report by the Wildlife Refuge states that all of the fresh water ponds on the island were filled with salt water.

Hurricane Carmen, a Category 3 storm, came ashore along the Louisiana coast near New Orleans on September 8, 1974. Although the storm hit 550 km away, tides on the island were 1 to 1.5 m above normal and wind gusts reached 65 km/hr.

In September 1975, Hurricane Eloise came ashore in Northwest Florida. The 1975 Annual Report for the island is missing from the files, so the effects the island experienced are unknown. The hurricane was classified as Category 3 and came ashore between Ft. Walton Beach and Panama City, approximately 80 kilometers west of St. Vincent Island. Tides in the area of impact were 3-5 m above normal and wind gusts were estimated to be 200-250 km/hr (National Hurricane Center). This storm most likely had a significant impact on St. Vincent Island.

The next hurricane to impact St. Vincent occurred on September 13, 1979. Hurricane Frederic, a Category 3 storm, came ashore just west of the Florida-Alabama border (National Hurricane Center). The main impact on the island came in the form of rainfall. Approximately 35 cm of rain fell following the hurricane. The culvert that connects Oyster Pond to the ocean was knocked out. The hurricane contributed to the wettest September to date for the island.

The year with the most hurricanes on record to hit St. Vincent Island was 1985. The first to strike was Hurricane Elena on September 1. The eye of the storm passed just 15-25 kilometers south of St. Vincent Island. Winds were recorded up to 200 km/hr,

making this a Category 3 hurricane. In addition to heavy rains, a funnel cloud passed through the area. The pattern of fallen trees indicated that winds came in from the northeast. Tropical Storm Juan traveled through the area in October. The main effect to the island was the 28.44 cm of rainfall. Hurricane Kate hit the island on November 21. This Category 2 storm moved directly across the island from the south. Storm surges were recorded to be 2-3 m above normal. The combination of these three storms caused some of the worst recorded damage the island has ever experienced.

Another year of numerous hurricanes was 1995. Hurricane Allison made landfall on June 5 at Alligator Point, approximately 30 kilometers to the east. Although the storm registered as Category 1, it did not have any physical impact on the island. Hurricanes Erin (Category 2) and Opal (Category 3) both made landfall at Pensacola Beach, approximately 125 miles to the west. The combination of these three hurricanes caused beach erosion and maintenance problems on St. Vincent Island. Opal, specifically, washed out several water control structures at unknown locations put in by the Wildlife Refuge.

Ho and Myers (1975) performed a study on the storm-tide height frequency for Franklin County, FL., which includes St. Vincent Island. Using the model developed by Overland (1975), they predicted the recurrence frequency for different storm surge heights in Apalachicola (Table 2-2), which can be compared to those experienced on St. Vincent Island. St. Vincent Island has experienced storm surge heights greater than 3 m twice since 1885, which is greater than the predicted recurrence interval. Due to unavailable data, it is not possible to determine if the island has experienced other intense storms at higher recurrence intervals than those predicted.

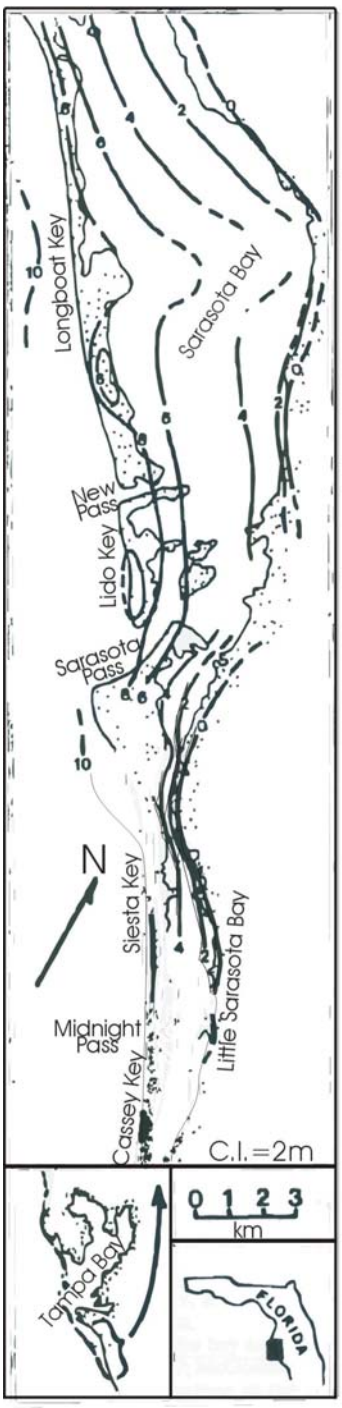

Figure 2-1. Location map of the two coastal bays studied by Davis et al. (1989) along the west-central coast. Contours are the pre-Pleistocene surface. Figure drafted from an article by Davis, R.A., Knowles, S.C. and Bland, M.J. (1989) Role of Hurricanes in the Holocene Stratigraphy of Estuaries – Examples From the Gulf Coast of Florida. *Journal of Sedimentary Petrology*, **59** (6), pg. 1053.

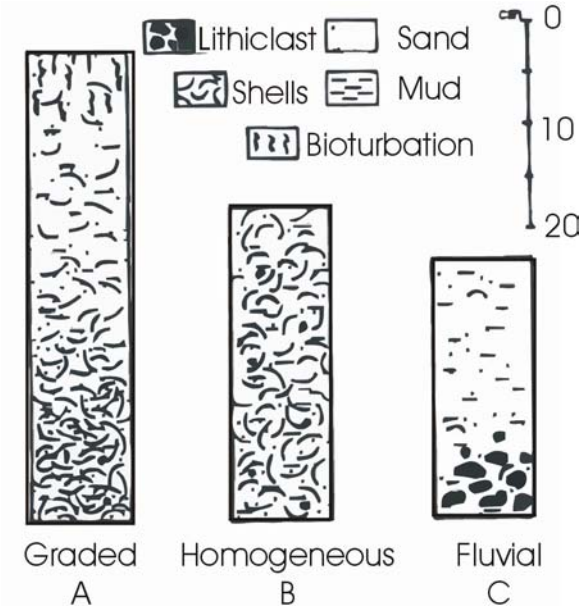

Figure 2-2. Diagram of the three storm facies. The graded facies is the result of intense storm activity and is characterized by abundant shells fining upward. The homogeneous facies is stratigraphically homogeneous and is the result of strong frontal passages or weak hurricanes. The fluvial facies contains abundant mud and gravel due to extreme rainfall. Figure drafted from an article by Davis, R.A., Knowles, S.C. and Bland, M.J. (1989) Role of Hurricanes in the Holocene Stratigraphy of Estuaries – Examples From the Gulf Coast of Florida. *Journal of Sedimentary Petrology*, **59** (6), pg. 1057.

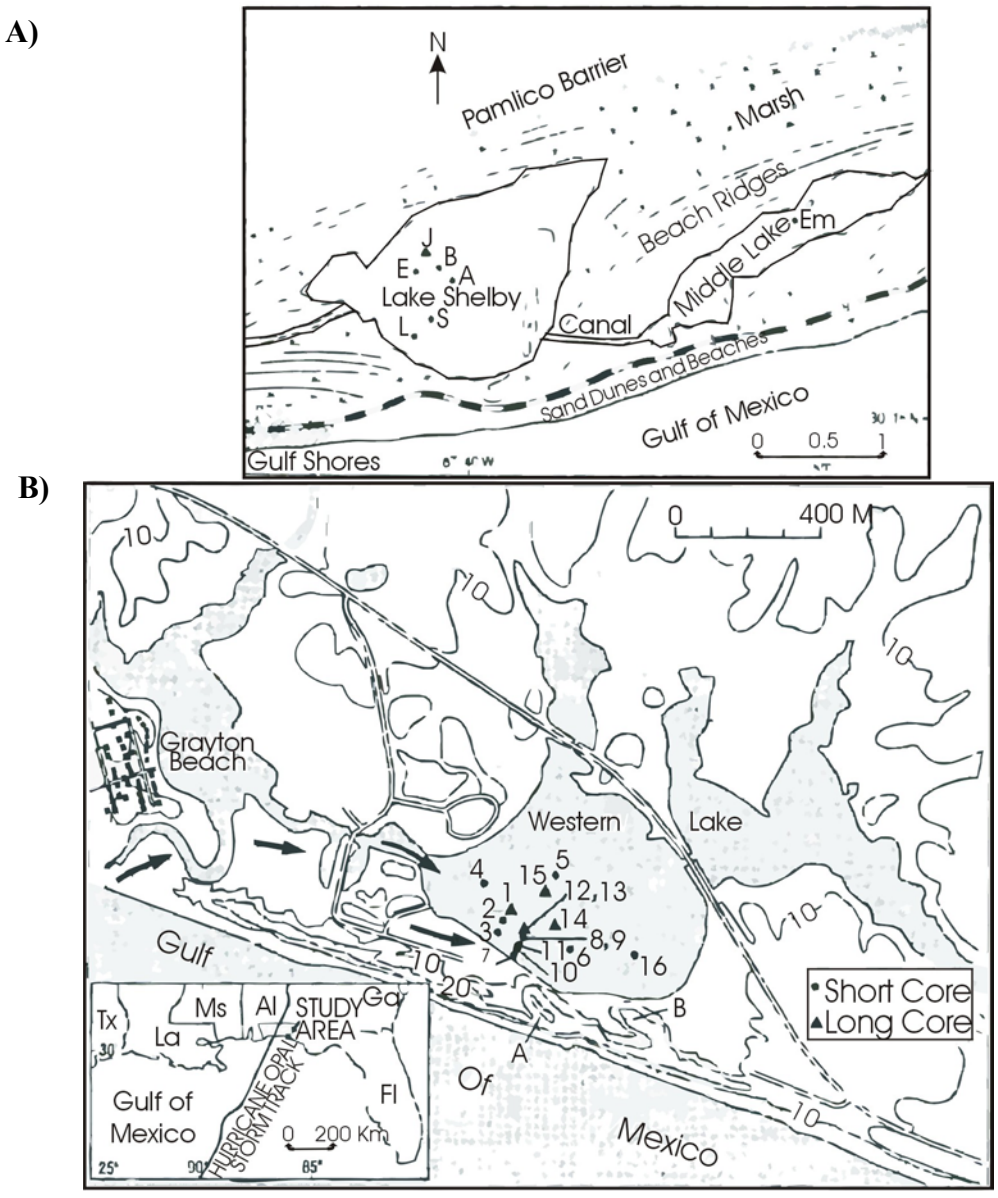

Figure 2-3. Location map for cores taken at A) Lake Shelby and Middle Lake, Alabama and B) Western Lake, Florida. Figures drafted from articles by A) Liu, K.B. and Fearn, M.L. (1993) Lake-sediment record of late Holocene hurricane activities from coastal Alabama. *Geology*, **21**, pg. 793 and B) Liu, K.B. and Fearn, M.L. (2000) Reconstruction of prehistoric landfall frequencies of catastrophic hurricanes in northwestern Florida from lake sediment records. *Quaternary Research*, **54** (2), pg. 238.

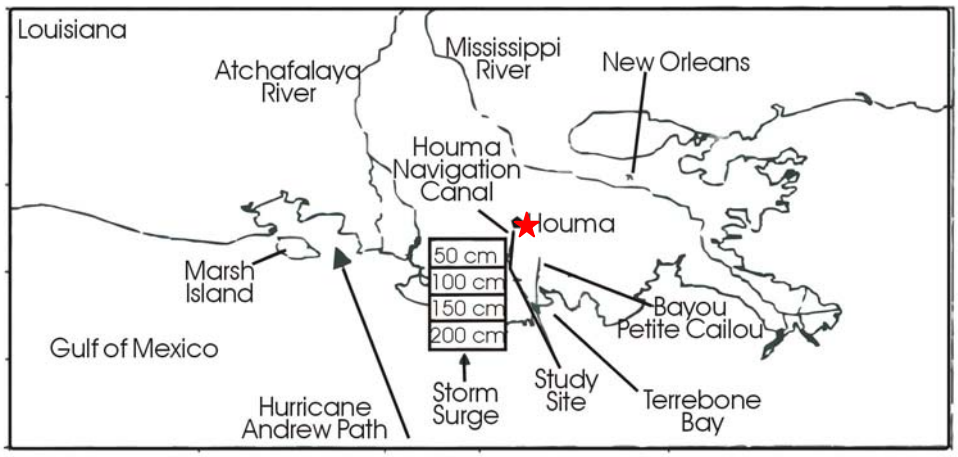

Figure 2-4. Location map of a study of coastal Louisiana hurricane deposits in salt marshes. Star indicates area where cores were taken. Figure drafted from an article by Parsons, M.L. (1998) Salt marsh sedimentary record of the landfall of Hurricane Andrew on the Louisiana coast; diatoms and other paleoindicators. *Journal of Coastal Research*, **14** (3), pg. 939.

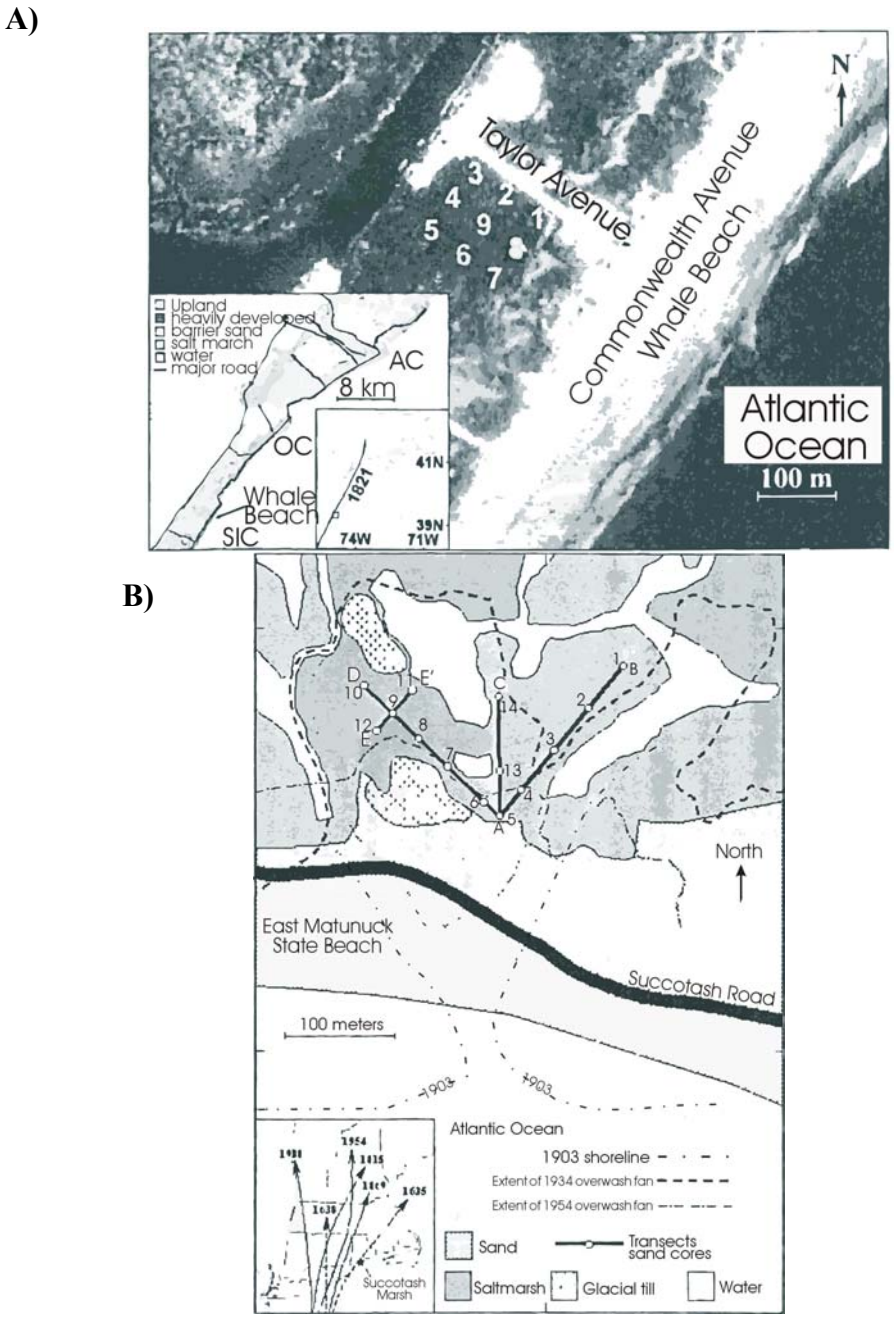

Figure 2-5. Location maps for cores taken in A) New Jersey and B) Rhode Island. Figures drafted from articles by Donnelly, J.P., Bryand, S.S., Butler, J., Dowling, J., Fan, L., Hausmann, N., Newby, P., Shuman, B., Stern, J., Westover, K., and Webb III, T. (2001a) 700 year sedimentary record of intense hurricane landfalls in southern New England. *Geological Society of America Bulletin*, **113** (6), pg. 714 and Donnelly, J.P., Roll, S., Wengren, M., Butler, J., Lederer, R., and Webb III, T. (2001b) Sedimentary evidence of intense hurricane strikes from New Jersey. *Geology*, **29** (7), pg. 615.

Table 2-1. Data on hurricanes to affect St. Vincent Island from 1880 to 2001 (St. Vincent National Wildlife Refuge, Williams and Duedell 1997, and Weather Underground 2003).

YEAR	Name	Category	Storm Surge (m)	Wind Gusts (km/hr)	Effects
1885	N/A	TS	N/A	80	N/A
1885	N/A	1	N/A	130	N/A
1886	N/A	5	N/A	N/A	N/A
1886	N/A	2	N/A	135	N/A
1894	N/A	3	N/A	170	N/A
1898	N/A	1	N/A	115	N/A
1899	N/A	1	0.91-1.22	130	N/A
1903	N/A	3	N/A	160	N/A
1915	N/A	1	N/A	145	N/A
1924	N/A	1	N/A	130	N/A
1926	N/A	3	N/A	200	N/A
1929	N/A	2	N/A	170	N/A
1939	N/A	1	N/A	130	N/A
1941	N/A	2	N/A	180	N/A
1966	Alma	N/A	N/A	N/A	N/A
1968	N/A	TS	N/A	100	N/A
1972	Agnes	1	1.88	N/A	All freshwater ponds filled with salt water
1974	Carmen	3	1.22	65	N/A
1975	Eloise	3	3.64-4.86	200-250	N/A
1979	Frederic	3	N/A	N/A	34.2 cm of rain, Culvert between Oyster Pond and the ocean knocked out.
1985	Elena	3	N/A	200	Fallen trees

Table 2-1. Continued

YEAR	Name	Category	Storm Surge (m)	Wind Gusts (km/hr)	Effects
1985	Juan	TS	N/A	N/A	28.44 cm rain
1985	Kate	2	2.43-3.03	N/A	N/A
1995	Allison	1	N/A	N/A	Beach erosion
1995	Erin	2	N/A	N/A	"
1995	Opal	3	N/A	N/A	Washed over several water control structures

Table 2-2. The predicted recurrence interval based on the model developed by Overland (1975) for storm surge heights of 4, 3, 2.5, and 1 m for comparison to the storm surges observed on St. Vincent Island.

Storm Surge Height (m)	Recurrence Interval (y)
4	500
3	100
2.5	50
1	10

Data from an article by Ho, F.P. and Myers, V.A. (1975) Joint probability method of tide frequency analysis applied to Apalachicola Bay and St. George Sound, Florida. NOAA Technical Report NWS 18, pg. 22.

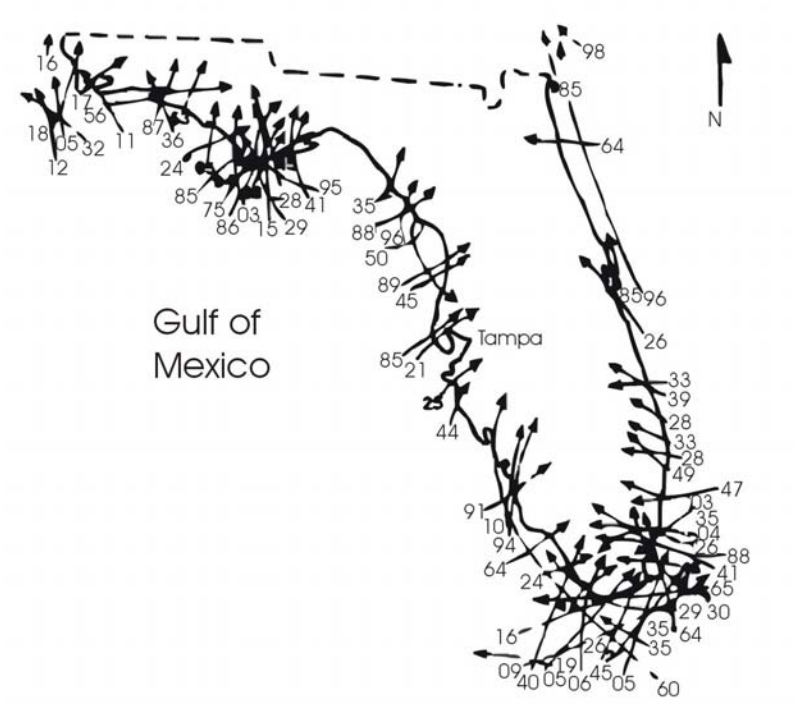

Figure 2-6. Figure showing that 56% of the hurricanes to strike the Florida panhandle from 1885 to 1994 hit in the Apalachicola Bay area. Figure drafted from an article by Davis, R.A. (1995) Geologic imapact of Hurricane Andrew on Everglades coast of Southwest Florida. *Environmental Geology*, **25** (3), pg. 145.

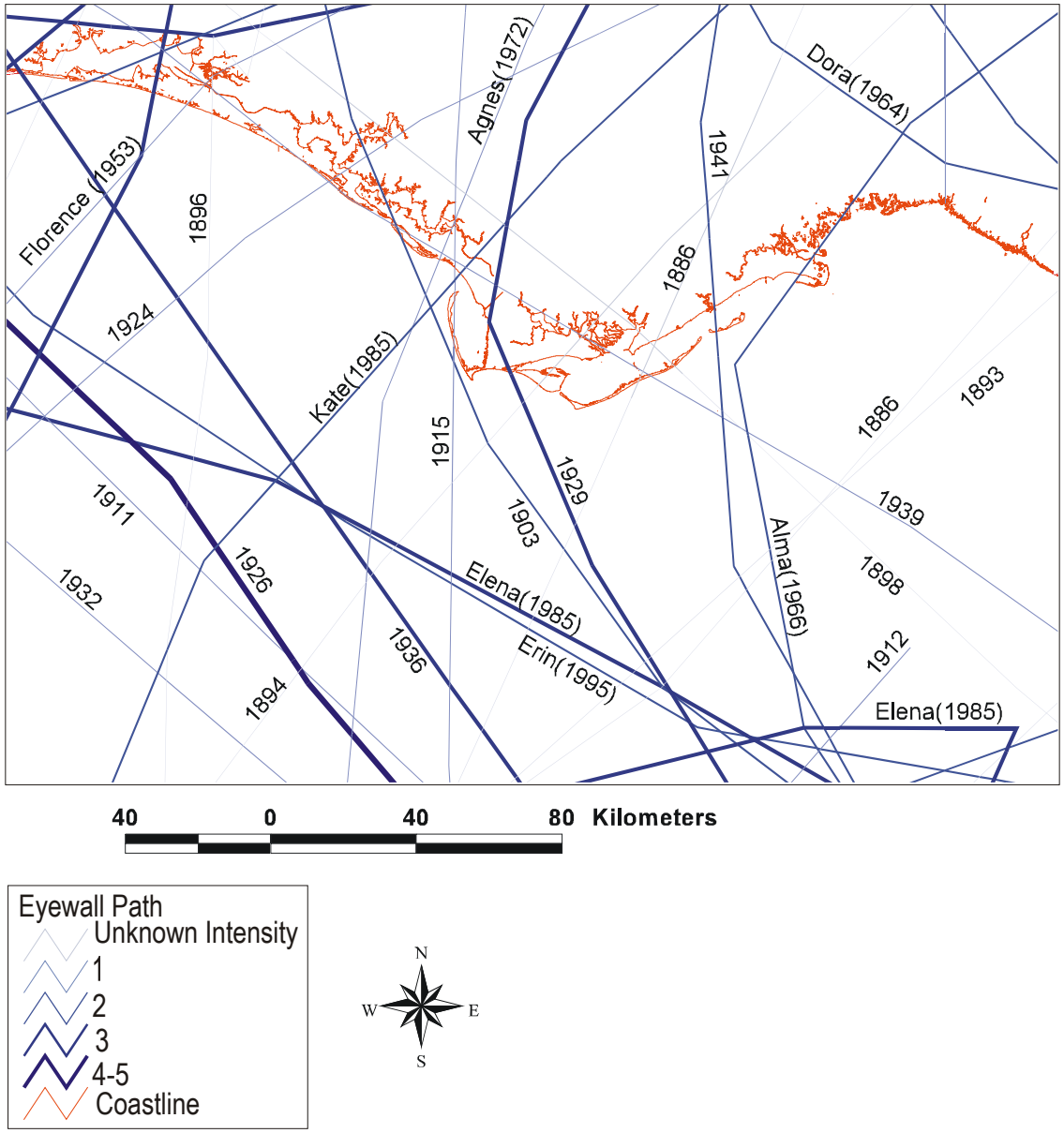

Figure 2-7. Path of hurricane eyewalls passing near St. Vincent Island (1885-1995). Numbers indicate the category of the storm according to the Saffir Simpson Scale.

CHAPTER 3
METHODS

The purpose of the sampling techniques used in this project is to provide information on the thickness of storm deposits, their sedimentological, geochemical, and micropaleontological properties, and the mechanisms of preservation of these deposits in the sedimenty record. Five piston cores were taken from St. Vincent Island using the coring method developed by Fisher et al. (1992). Cores approximately seven centimeters in diameter were taken from Flag Pond (2) and Oyster Pond (2) (Figure 3-1). The length of these cores ranges from 57 to 75 cm. Sampling locations on the island were chosen based on the proximity of the pond to the coast as shown in Landsat TM imagery and accessibility by car and boat. Since both Oyster and Flag Ponds are only separated from the southern coastline of the island by dunes, they were assumed to have received the greatest amount of washover during a tropical storm or cyclone.

The cores were kept vertical during transport and stored at 4ºC. Once in the lab, the cores were analyzed for bulk density and magnetic susceptibility at 0.5 cm intervals using a Geotek Multi-sensor Core Logger. The accuracy of the bulk density measurements was determined by plotting the gamma counts/second (determined using a standard aluminum density calibration piece) versus density*thickness of the aluminum (Weber et al. 1997). Cores were then split and processed through the core logger for detailed digital imaging at a resolution of 40 pixels/cm. Next the cores were x-radiographed at 50 KeV/450 mAs to reveal internal structures and changes in sediment

density. The x-rays were scanned and then processed by SCION software to generate a relationship between the sediment density and the gray scale pixel density.

Following the non-destructive core analyses, both halves of each core were sampled at 1 cm intervals, which was the smallest interval that produced enough material for grain size and radioisotope measurements. Samples from one half of the core were divided and prepared for radioisotopic dating, stable isotope analyses, and pore water analyses. Samples from the other half of the core were reserved for grain size and microfossil analyses.

Particle-reactive radioisotopes are used in sedimentological studies to examine sediment mixing and accumulation rates (Appleby and Oldfield 1992) and to distinguish event beds preserved in the geologic record (Jaeger and Nittrouer 1999). Samples for radiometric dating were freeze dried, powdered, packed into plastic tubes with up to 3 cm of dry sediment, and then sealed with a mix of epoxy resin. The activity of naturally occurring radioisotopes was measured with well-type intrinsic germanium detectors (Schelske et al. 1994). A large range of γ-energies were counted for 24-48 hours depending on sample height for a minimum of 380 counts to reduce the counting error to <5%. The activity of ^{210}Pb, a decay product of ^{226}Ra in the ^{238}U decay series, was measured in each sample. The samples were set aside for a minimum of three weeks to establish secular equilibrium between radon (^{222}Rn) and radium (^{226}Ra). The excess activity of ^{210}Pb was determined by subtracting the supported ^{210}Pb (^{210}Pb in secular equilibrium with ^{226}Ra) from total ^{210}Pb activities. The activity of ^{137}Cs, which may be used as an additional age marker, was also determined. Sample mass and height and counting efficiency (98-99%) were factored into calculations of activity of each

radionuclide (Schelske et al. 1994). Blanks were counted before and after measurements of each core in order to determine background radiation. Amersham International standards of Americium-241 and Cesium-137 were run within one year of the measurements. Standards do not have to run before or after each set of samples due to the 98-99% efficiency of the well detector. The counting error is measured as the square root of the number of counts for each sample.

The weight percent carbon and nitrogen concentrations were determined with a Carlo-Erba Elemental Analyzer on one-centimeter subsamples. Approximately 3-5 mg of sample were placed in tin cups and dried under a heat lamp. Combustion of samples at 1000ºC determined the total carbon and nitrogen. Four Atropine standards with a specific percent of carbon and nitrogen were run before each set of samples to determine a regression line to relate the size of the samples to the percent carbon and nitrogen in each one. The precision of the analyses was determined by analyzing duplicates of every tenth sample. The relative percent difference (RPD) was determined using the formula: $(|x_1-x_2|)/x_{mean}$. The RPD for %C was calculated to be ±6.4% and the RPD for %N was ±5.5%.

Samples for pore water analyses were centrifuged to separate sediment and water. Salinity analyses on the porewater were performed using a portable refractometer. Standard precision and accuracy of portable refractometers is ~1 ppt.

Samples for grain size and microfossils were wet-sieved at 63 μm to separate the sand and mud-sized fraction. Sand-sized particles were dried in an oven at 60ºC. Approximately 0.5 to 1.5 grams of each sample were analyzed on an automated settling column for grain size measurements (Syvitski et al. 1991). The settling column method

measures grain size as a function of settling velocity, assuming a spherical particle shape. The results are reported numerically as the percent of the total mass at each phi size class (0.1Φ), mean, median, mode, and sorting. The accuracy of the automated settling column was determined with NIST Standard Reference Material glass beads. The precision of the instrument was determined by running duplicate samples. The RPD for median was calculated to be ±0.5%, ±0.7% for mean, ±4.3% for mode, and ±4.7% for sorting.

The percent sand for each sample was estimated based on the difference between the total weight of the sample before it was split into sand and mud fractions and the weight of the sand fraction after the sample was split by Equation 3-1:

$$\frac{\text{(Total Sample Weight Wet (g) – Water Weight (g) – Dry Sand Weight (g))}}{\text{Water Weight (g)}} = \%\ \text{Sand} \qquad (3\text{-}1)$$

The water weight for each sample was determined by the following equation:

Total Sample Weight Wet (g) * % Water = Water Weight (g)

The percent water was calculated based on the weight of the samples from the archive core before and after they were freeze dried by Equation 3-2:

$$\frac{\text{Total Sample Weight Wet (g)} - \text{Total Sample Weight Dry (g)}}{\text{Total Sample Weight Wet (g)}} * \text{Water Density} = \%\ \text{Water} \qquad (3\text{-}2)$$

Water density was presumed to be 1.03.

Because marine macrofossils and microfossils in terrestrial sediments are useful indicators of hurricane deposition (Collins et al. 1999, Davis et al. 1989, Parsons 1998), biostratigraphic measurements were done on each 1-cm sample. A portion of each sand-sized sample was split to 0.15-0.30 g and microscopically analyzed for foraminiferal classification and abundance. All of the forams in each sample were picked, mounted, and identified by comparison to known fresh and saltwater groups at the genus level.

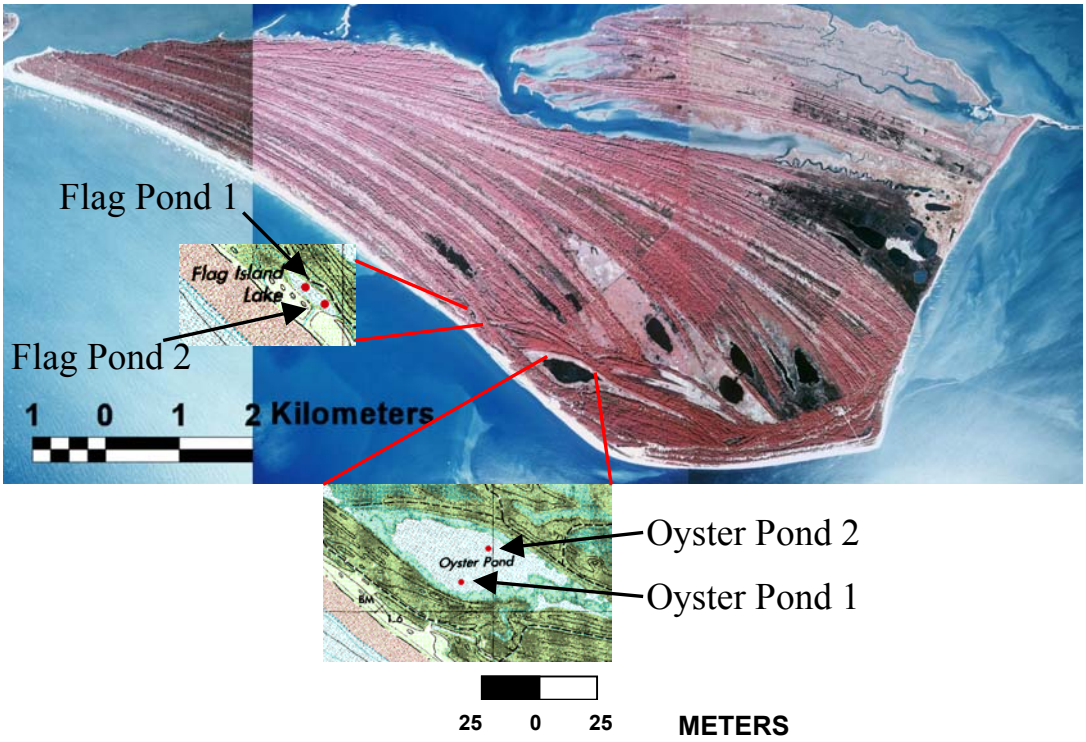

Figure 3-1. Coring locations

CHAPTER 4
RESULTS

General Lithology

The digital photographs show the Oyster Pond cores to be relatively homogeneous in color and texture and dominated by muddy sediment with greenish color (Figure 4-1). Core OP1 has shifts in gamma bulk density at ~16 and 34 cm (Figure 4-2). A steady increase in bulk density down to 16 cm is followed by an interval of scattered values ranging from 1.2 to 1.4 g/cm^3. The values remain at a lower density from 34 to 54 cm with a gradual increase in bulk density below 54 cm. The red-green-blue color reflective data for this core shows a transition at ~14 cm from lower (lighter) to higher (darker) values (Figure 4-4). Small peaks occur at 24, 28, 34, and 50 cm. The blue data plots slightly lower than the red and green data. The gamma bulk density and red-green-blue data for core OP2 show an increase at 8 cm followed by a drop at 13 cm. There is also a peak in gamma bulk density at 58 cm (to 1.25 g/cm^3).

The Oyster Pond cores show several small bedding changes through visual and x-radiographic examination (Figures 4-1, 4-2, and 4-3), and the gamma bulk density measurements for OP1 reveal several small layers of higher density material at 22 cm and 34 cm. The large increase in bulk density at 34 cm is related to a large mollusk shell found at that interval.

The gray scale pixel intensity data from digitized x-radiographs for core OP1 indicate layers with darker (pixel density of >30 than surrounding data) gray scale pixel values at 13-15 (a slanted layer), 19, 23, and 36-37 cm (Figure 4-6). The gray scale pixel

intensity data for core OP2 is highly variable, with layers of darker pixel values at 8,17, and 23-24 cm. Values gradually increase from 21 cm to the bottom of the core. Lighter pixel values appear to correspond with higher density material (Figure 4-7).

The two cores from Flag Pond have one major change in color and texture downcore (Figure 4-1). The digital photographs show an abrupt switch from darker sediment to lighter sediment at 12 cm (FP1) and 20 cm (FP2). The Flag Pond cores are very sandy (~60-90% sand). The darker sediment is concentrated near the surface (Figure 4-1). At ~14 cm, core FP1 transitions from mud-rich to a sandier texture, with corresponding increases in gamma bulk density (from ~1.1 to 1.6 gm/cc) and red-green-blue data (Figures 4-4 and 4-5). The gamma bulk density for core FP2 does not show a change in sediment character until ~38 cm. The values for bulk density increase from ~1.1 to 1.6 gm/cc, but they do not remain constant after the increase (i.e., there are some sand and mud layers mixed together). Other minor changes in density occur at 20, 29, 39, and 48 cm. The red-green-blue data shows a shift from darker to lighter values at ~20 cm and small peaks at 9, 14, 29, and 40 cm. Both cores FP1 and FP2 plot the blue data at lighter values, followed by green, and then red at darker values.

The photographs of core FP2 show changes from dark to light at 13 cm (Figure 4-1). The x-radiographs from both Flag Pond cores do reveal several gradual bedding changes (Figure 4-6). Core FP1 has a contact ~11 cm below the surface, with a corresponding increase in the bulk density at this same depth. The x-radiographs reveal pronounced contacts in core FP2 at 26 cm, 38 cm, and 48 cm, with corresponding increases in gamma bulk density at 38 cm and 48 cm. All of these are sharp contacts with definite associated color and lithology changes.

The gray scale pixel data for core FP1 shows a diffuse contact between light and dark material from 14 to 16 cm (Figure 4-6). Other variations in pixel data occur at 6, 21, 24.5, and 27 cm, and all of these intervals represent slight variations in density and would only be detected through detailed analysis at <1 cm sampling intervals. The gray scale pixel data for core FP2 show the same change in lithology at ~24-25 cm that is seen in core FP1 that reflects a transition from light to darker sediment. The gray scale pixel data also reveals laminations at 11, 14, 19, and 33 cm. The increase in pixel density at 33 cm appears to be a small bed of lower density material.

^{210}Pb Analyses

Measurements of ^{210}Pb for core OP1 reveal supported ^{210}Pb at 18-19 cm (Figure 4-8). Total ^{210}Pb activities varied from 2.0 dpm/g to 5.5 dpm/g. Excess ^{210}Pb activities range from 0.5 dpm/g to 5.5 dpm/g. Excess activity decrease fairly steadily downcore with the exception of small increases at the 10-11 cm and 13-15 cm intervals.

Core FP1 contains variations in the ^{210}Pb activities downcore with no discernible trend (Figure 4-8). The measurements of total and excess ^{210}Pb activity range from 0.0 dpm/g to 5.0 dpm/g. Samples at 0.5, 2.5, 4.5, and 5.5 cm have higher activities (5.0 dpm/g decreasing downcore to 1 dpm/g), while samples at 1.5 and 3.5 cm have activities of <1 dpm/g.

Core FP2 also shows down core variations in ^{210}Pb activity (Figure 4-9). Total ^{210}Pb is greatest at the top of the core (9 dpm/g at 0.5 cm). Excess ^{210}Pb activity is 7.5 dpm/g at the top of the core and decreases to 0.5 dpm/g at approximately 30 cm. Measurements are missing for several depths because analyses were done on this core only for the purpose of estimating the depth of supported ^{210}Pb.

^{137}Cs Analyses

Measurements of ^{137}Cs activity are used as a complementary dating tool to ^{210}Pb because it has a unique source (atomic weapons tests) that overlaps the period of ^{210}Pb dating (~100 years). Unless mixing has occurred, the depth in the core that first shows ^{137}Cs activity should correspond to 1954.

Core OP1 has a downcore decreasing ^{137}Cs activity profile that reaches 0.0 dpm/g at a depth of 12 to 13 cm (Figure 4-10). There is a minor decrease in activity at the 2-3 cm depth interval. The ^{137}Cs activity profile for core FP1 does not reveal the same decrease with depth as core OP1. There is a decrease in activity from 1-2 cm that corresponds to a ^{210}Pb decrease. The profile for ^{137}Cs for core FP2 (Figure 4-11) also shows variation in activity with depth, with higher activity of 2.0 dpm/g at 10.5 cm, 0.6 dpm/g at 16.5 and 17.5 cm. Measurements of ^{137}Cs activity remain at 0.0 dpm/g for both 20.5 and 29.5 cm.

Magnetic Susceptibility

The magnetic susceptibility sensor records raw data and does not account for density changes downcore. Data may reflect changes in density rather than magnetic susceptibility, therefore, the data have been mass corrected by the following equation:

$$X = K/\rho \qquad (4\text{-}1)$$

where X is the mass specific susceptibility, K is the uncorrected susceptibility, and ρ is the sediment density. Units for susceptibility are 10^{-6} cgs.

Core OP1 does not have any high amplitude peaks in magnetic susceptibility (Figure 4-12). It does, however, have a steady increase from 5 cm to 10 cm and then declines gradually below this point with minor increases at 35 and 41 cm. Core OP2 has one large peak at 16 cm, declines until ~25 cm, and remains steady downcore.

Both Flag Pond cores display two large magnetic susceptibility peaks (Figure 4-12). For core FP1, the peak at 17 cm has a maximum value of $1.3^{x}10^{-6}$ cgs and the peak at 27 cm has a maximum value of $1.9^{x}10^{-6}$ cgs. The peaks for core FP2 are at 24 and 37 cm. The peaks are separated downcore by 10-15 cm in both cores, but are offset 8-10 cm between cores.

Grain Size

All grain size measurements were performed on 1 cm intervals (Figures 4-13, 4-14, and 4-15). The mean, median, sorting, and mode were calculated for the sand fraction (>63μm) based on measurements from an automated settling column (Syvitski et al. 1991) (Figures 4-14 and 4-15). Measurements were only performed on the sand as it contains the most relevant information about overwash processes. Because there are no measurements for samples that were too small in mass to be run on the settling column (< 0.5 g), core OP1 has missing data for the intervals of 1-2, 2-3, 7-8, 8-9, 9-10 and 16-17 cm and core FP1 has missing data for the intervals of 1-2, 3-4, 6-7, and 14-15 cm.

Peaks in mass percent sand for core OP1 occur at 2.5, 6.5, 19.5, and 27.5 cm (Figure 4-13). The mass percent sand for core FP1 shows a transition from a variable profile to a constant profile at 12.5 cm. Peaks occur at 2.5, 4.5 and 8.5 cm.

All samples in core OP1 contained less than 50% sand, with only three samples having greater than 40% sand (Figure 4-13). The data formed a trendline when percent sand was plotted against gamma bulk density (Figure 4-16). There were only five samples that did not fit the trendline (at 0.5, 1.5, 2.5, 3.5, and 8.5 cm). Core FP1 was the opposite of core OP1 and contained increased amounts of sand (40-60% greater) (Figure 4-13). Only four samples contained less than 50% sand, with the majority of the samples

containing greater than 75% sand. The plot of percent sand versus gamma bulk density showed two trends (Figure 4-16). Samples above 12 cm followed one trend while samples below 12 cm followed another.

The median and mean sizes of the sand fraction for core OP1 were finer than the median and mean for core FP1 (Figure 4-14). The measurements for core OP1 cluster around the average values for the south-facing beach (2.2 phi), while the measurements for core FP1 cluster around the average values for the ridge sands (1.9 phi). The mean values for core OP1 are slightly more scattered than the median values. Core FP1 shows very similar values for both median and mean.

Sand in core OP1 is moderately to moderately well sorted, with sorting values of ranging from 0.3 to 0.9 (Figure 4-15). There is not a consistent pattern downcore for sorting. Sand in core FP1 is also moderately to moderately well sorted and does not show any downcore variation. Neither core matches the sorting values calculated for the ridge sands, south-facing beach, and east-facing beach.

While the values for median, mean, and sorting are constant downcore for core FP1, the modal values are quite varied (Figure 4-15). Values range from 1.7 to 2.3 and there is no consistent downcore pattern. Modal values for core OP1 are uniform downcore with the exception of the sample from 13-14 cm. This sample has a very low value at 0.75. The modal values for this core cluster just above the values for the south-facing beach.

Micropaleontology

Both ponds show an absence of forams above 17 cm for core OP1 and 25 cm for core FP1 (Figure 4-17). Below these depths, the number of forams sharply increases to abundances greater than 100 forams per cm^3. Decreases to below 60 forams per cm^3

occur at 16, 22, 24, and 26 cm for core OP1 and at 27 and 29 cm for core FP1. Greater than 90% of the forams were identified as belonging to the *Ammonia* genus.

Salinity

Samples from every other centimeter from both ponds were put into a centrifuge and spun down to separate pore water. Samples from core FP1 were not sufficient to produce enough pore water to measure, so samples from core FP2 were used instead.

The salinity values for core OP1 range from 10 to 15 ppt with fluctuations near the surface (until 7cm depth), decreasing in amplitude with depth (Figure 4-18). These measurements are slightly higher than the overlying water (7 ppt). Core FP2 salinity values decrease steadily downcore from 17 to 26 ppt. The overlying water in Flag Pond has a salinity reading of 20 ppt.

Weight %C and %N

Concentrations of organic carbon and nitrogen track one another in cores OP1 and FP1 (Figure 4-19), but with respect to depth, the trends were different between the cores. In core OP1 the values decrease from 6.25 to 3 for %C until 5 cm and then leveled off at ~2%. The %N values decreased from 0.67 to 0.33% and then reached a constant level of 0.2%. Core FP1 had higher values for both elements (14-20% for carbon and 0.9-1.2% for nitrogen) than core OP1 towards the top of the core. Although there were minor variations with depth, the values remained constant and elevated until 10 cm. Below this depth, both the carbon and nitrogen values remained at 0% within the analytical precision of the instrument.

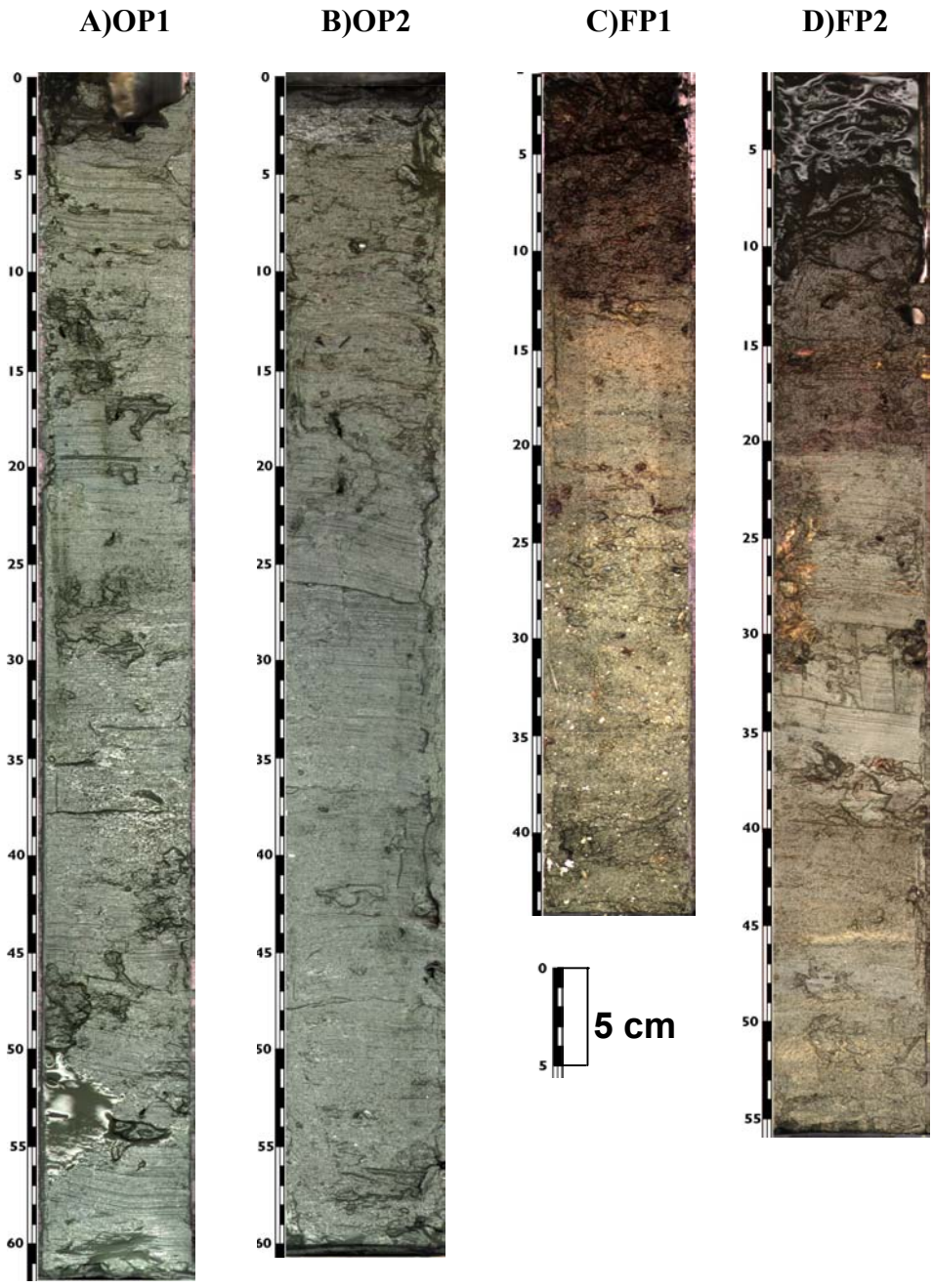

Figure 4-1. Photographs of cores A) OP1, B) OP2, C) FP1, and D) FP2.

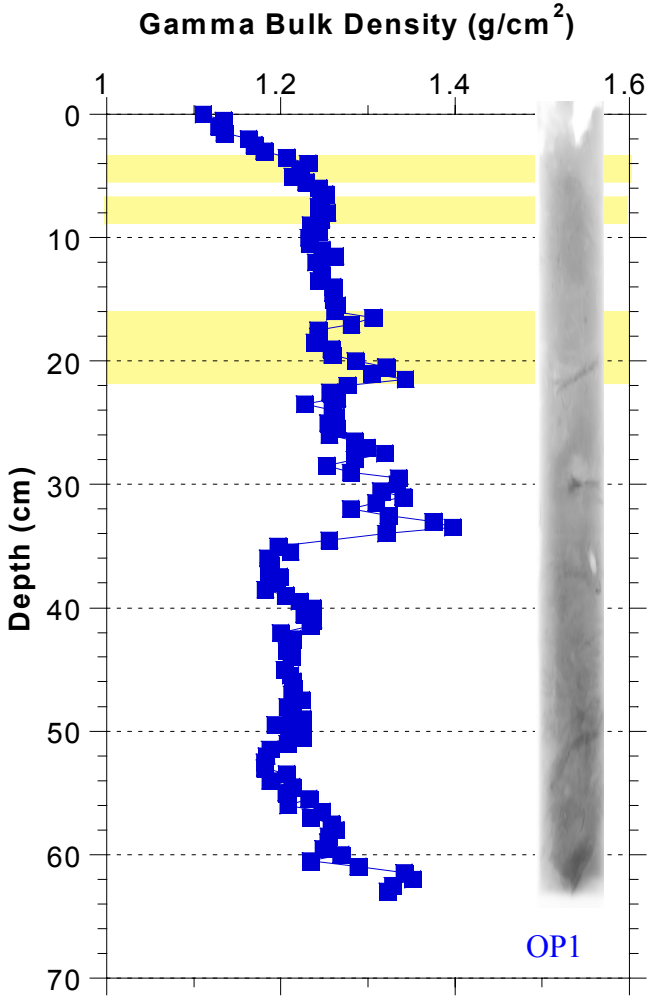

Figure 4-2. Gamma bulk density and x-radiograph data for core OP1. Yellow boxes represent depth matched to date of known hurricanes for OP1.

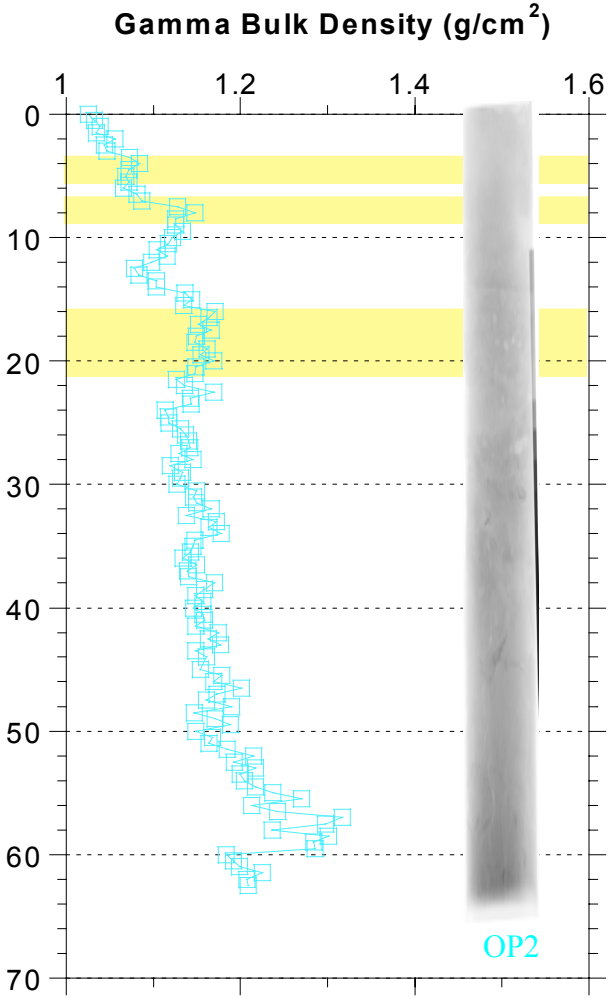

Figure 4-3. Gamma bulk density and x-radiograph data for core OP2. Yellow boxes represent depth matched to date of known hurricanes for OP1.

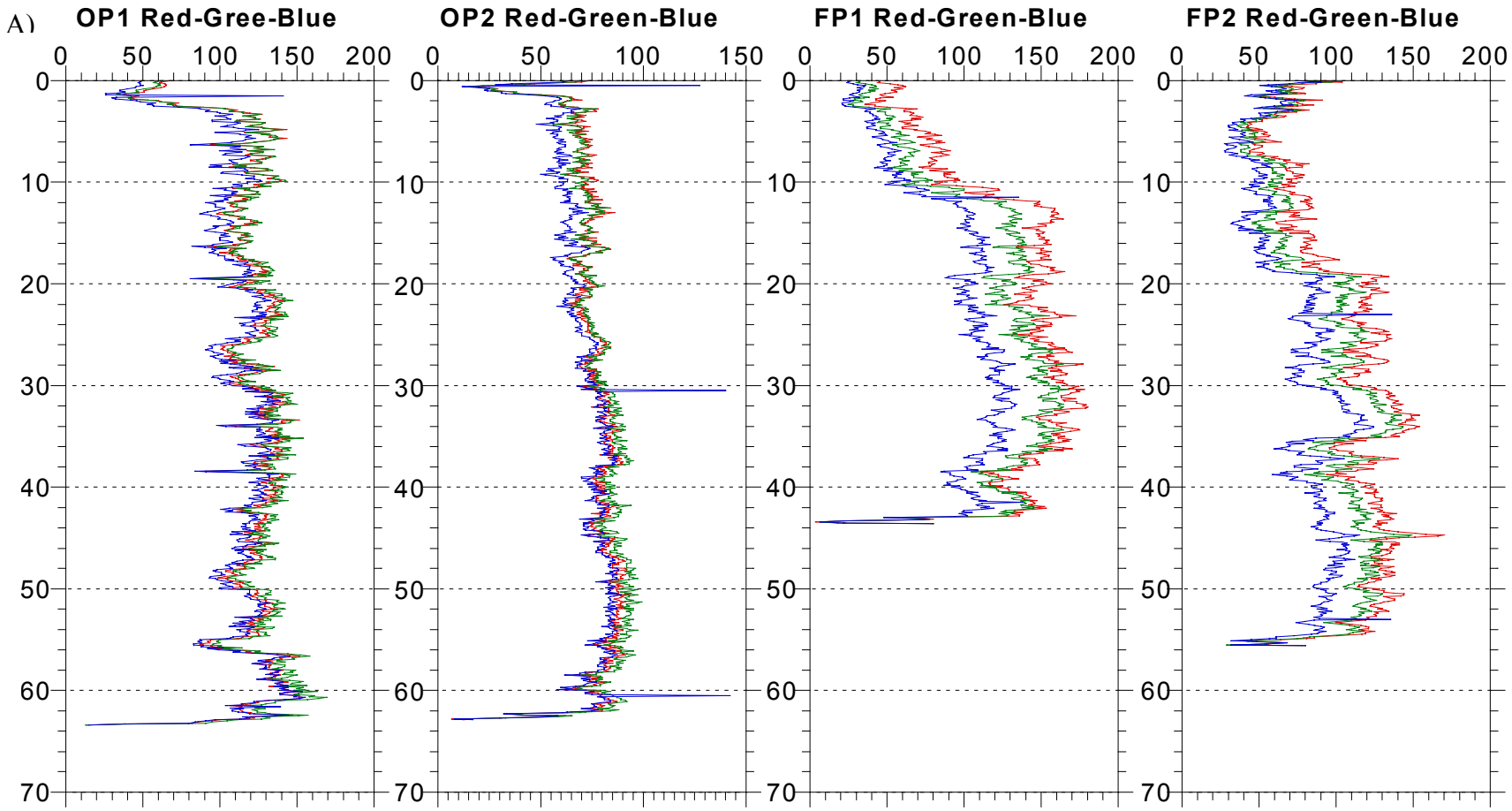

Figure 4-4. Red-green-blue data for cores A) OP1, B) OP2, C) FP1, and D) FP2. Increased values indicate darker sediment. The spikes in the blue values are an artifact of sampling and not relevant data.

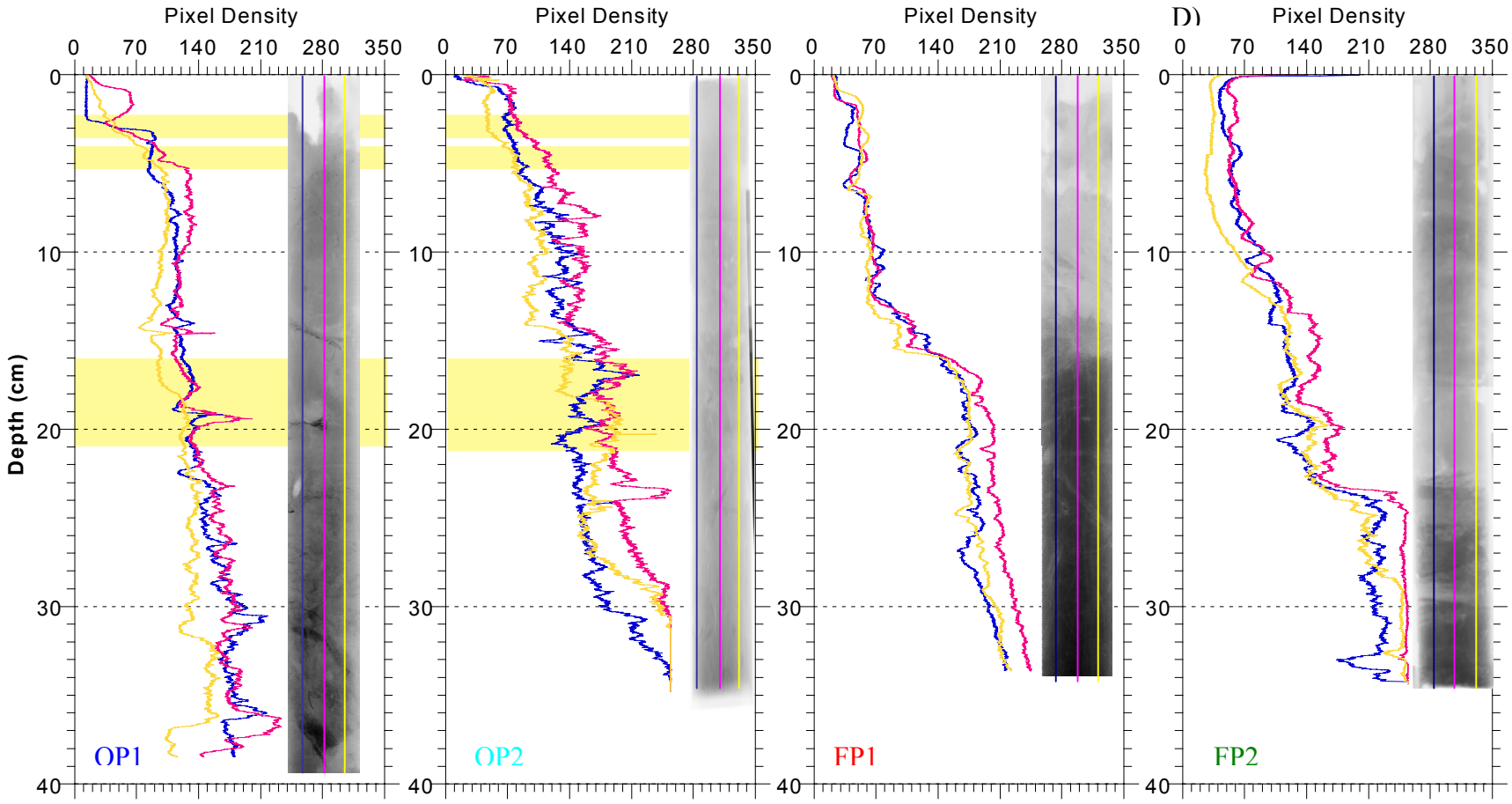

Figure 4-5. Pixel density and x-radiograph data for cores A) OP1, B) OP2, C) FP1, and D) FP2. Yellow boxes represent depth matched to date of known hurricanes for OP1.

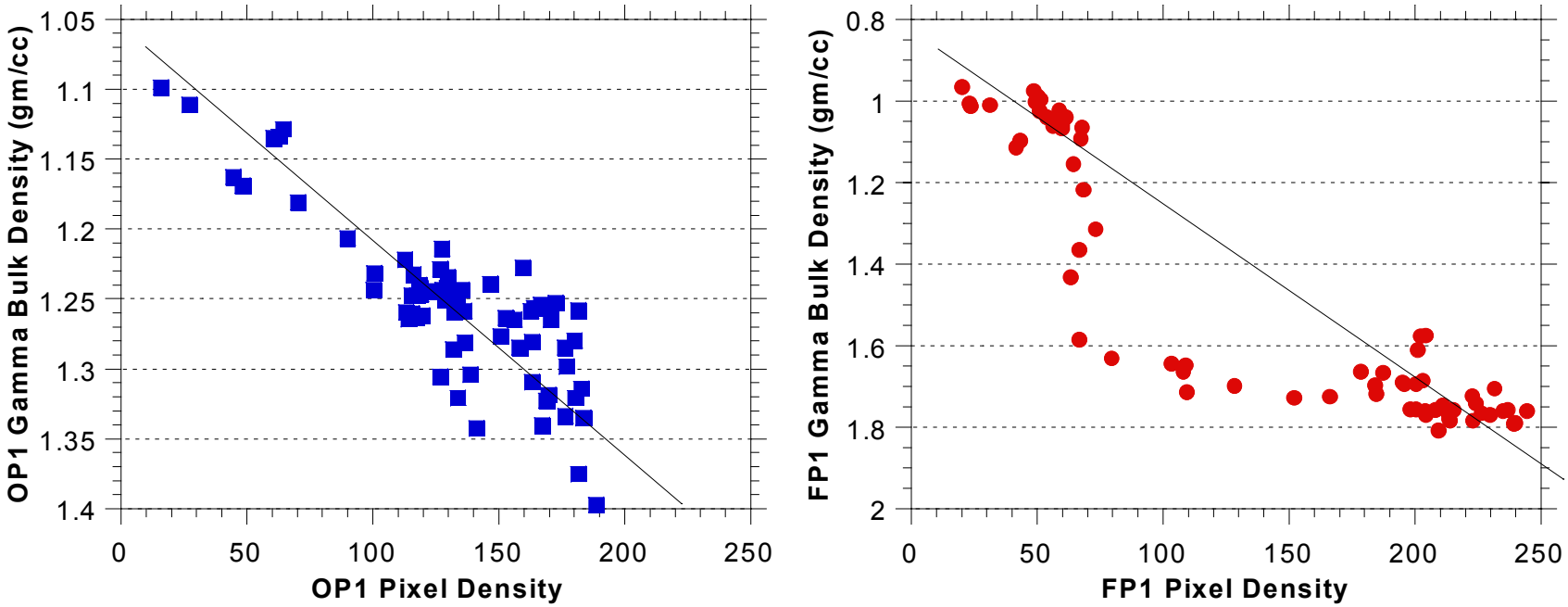

Figure 4-6. Plots of gray scale pixel density versus gamma bulk density for cores A) OP1 and B) FP1. Black lines represent trends in the data.

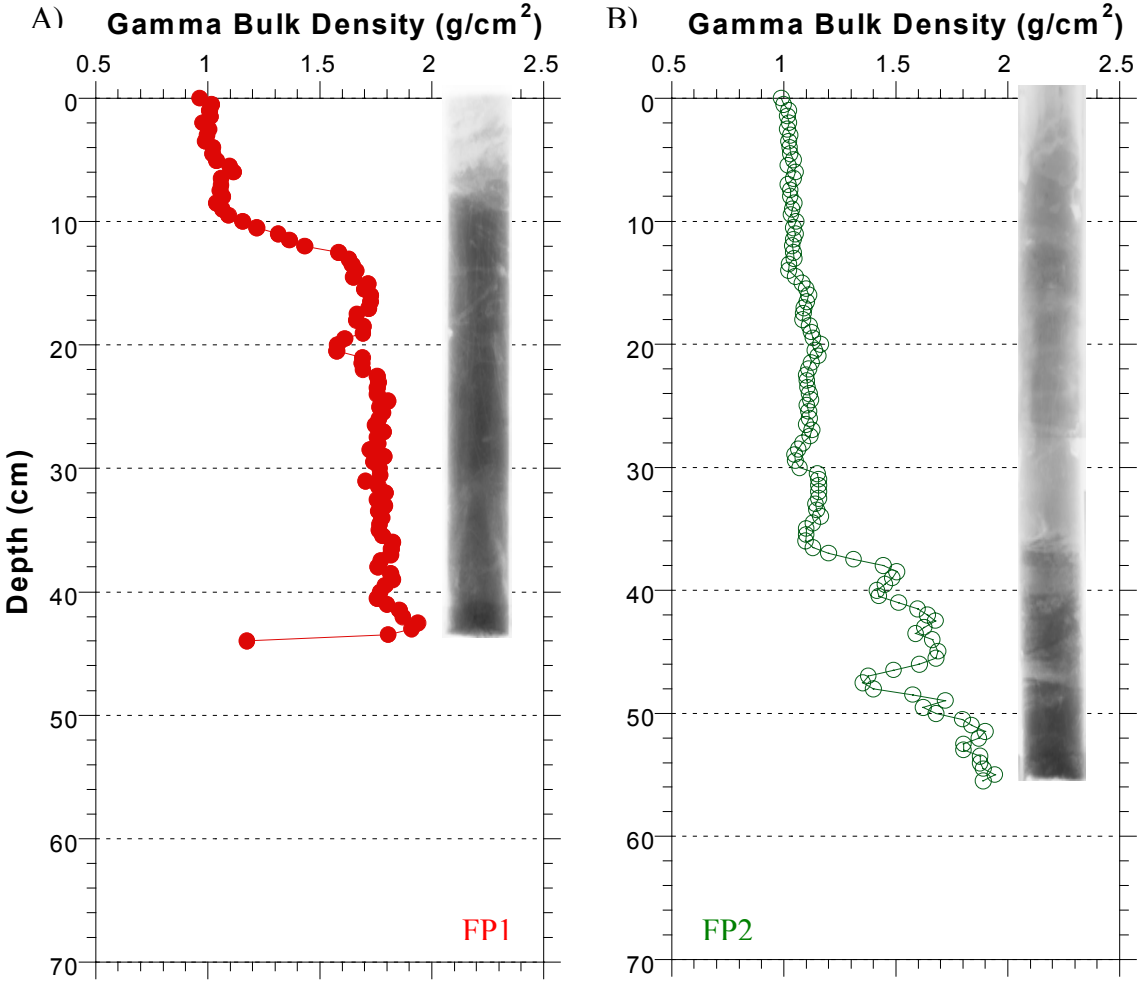

Figure 4-7. Gamma bulk density and x-radiograph data for cores A) FP1 and B) FP2.

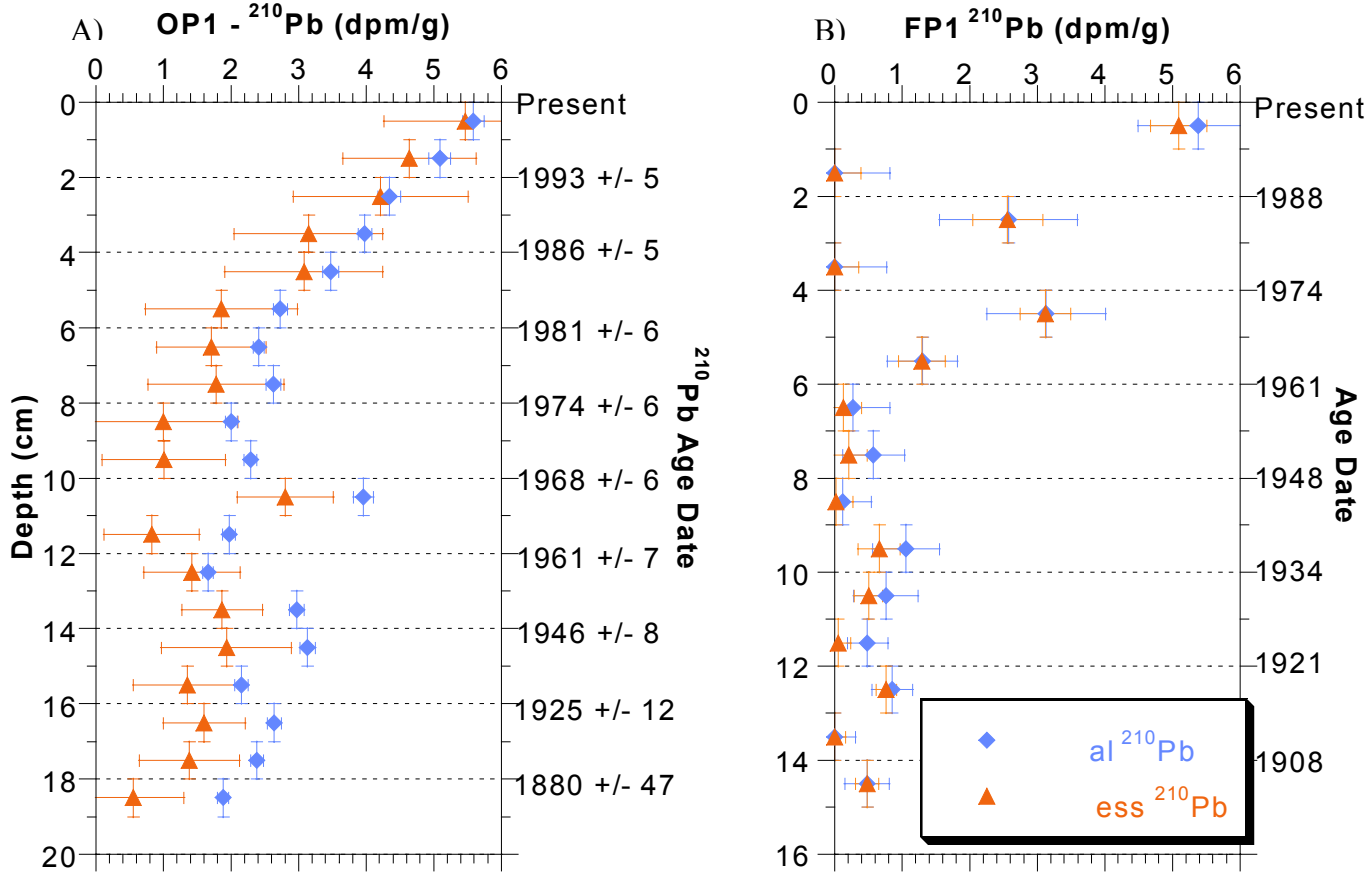

Figure 4-8. Total and excess ^{210}Pb activity for cores A) OP1 and B) FP1. Dates for core OP1 are calculated by the method developed by Binford (1990). Core FP1 dates are based on an approximated sediment accumulation rate of 1.5 mm/yr.

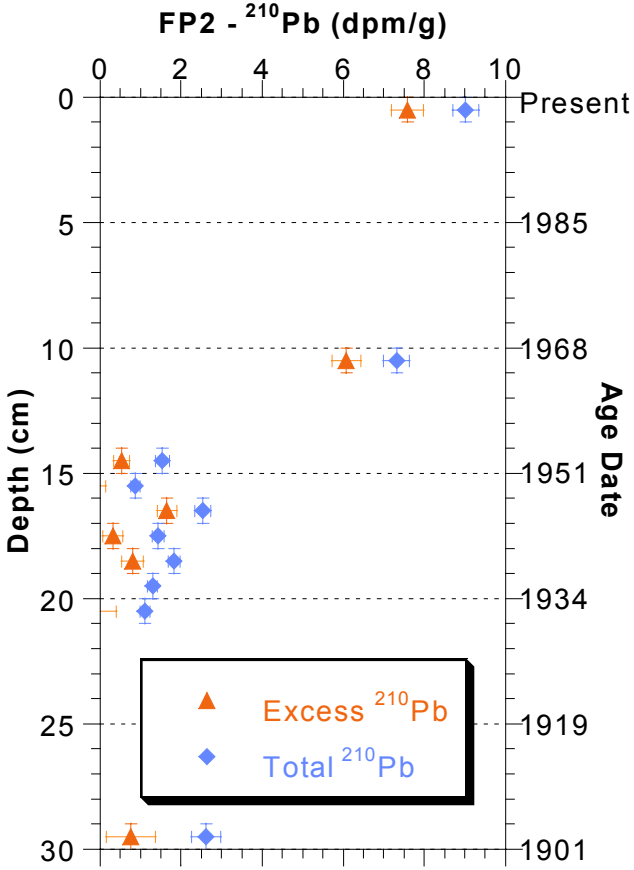

Figure 4-9. Measurements of total and excess ^{210}Pb for core FP2. Age dates are based on an approximated sedimentation rate of 3.0 mm/yr.

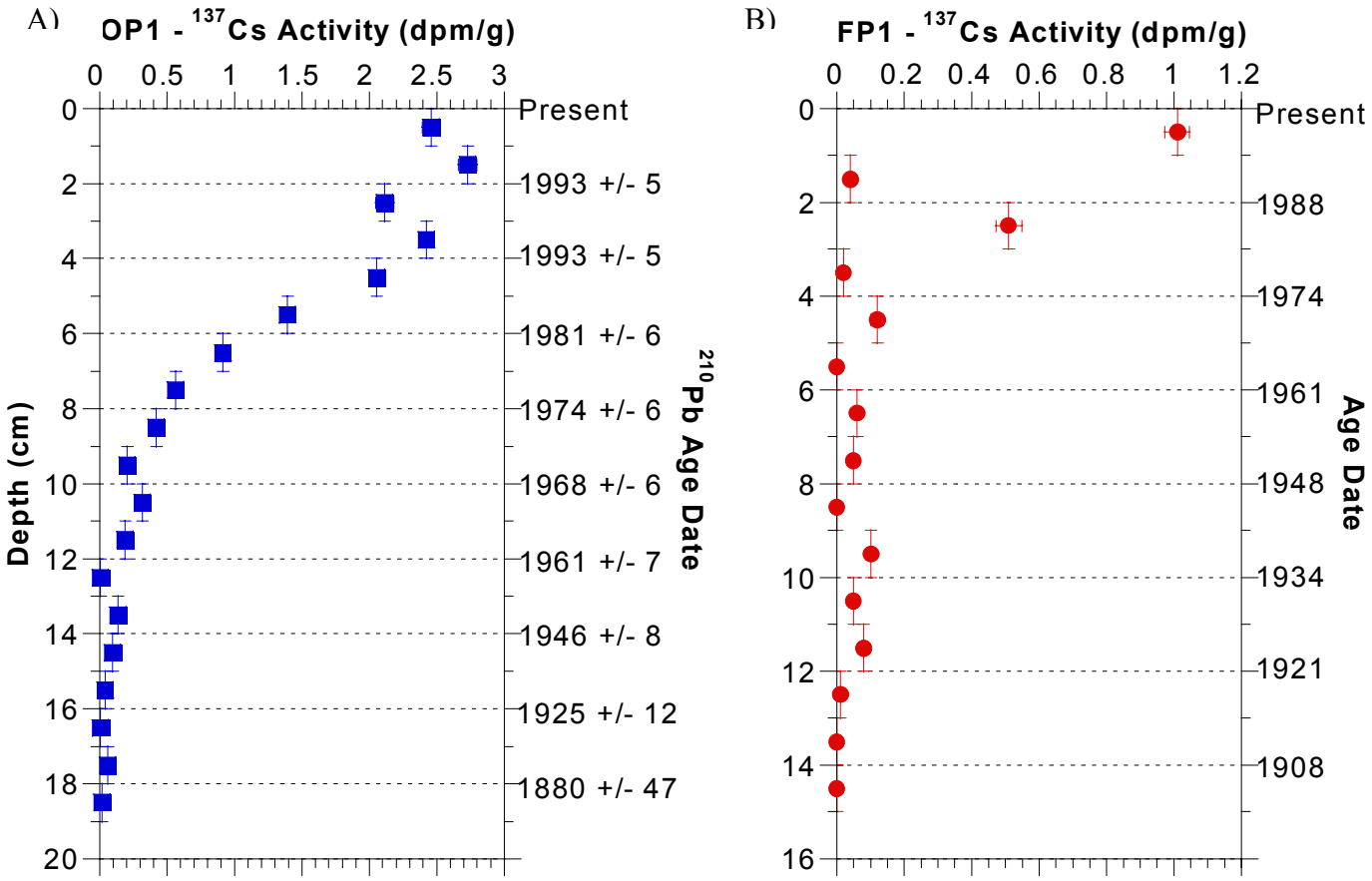

Figure 4-10. ^{137}Cs activity for cores A) OP1 and B) FP1. Age dates for core FP1 are based on an estimated sedimentation rate of 1.5 mm/yr. Activity goes to 0 dpm/g at 12 cm for both core OP1 and FP1.

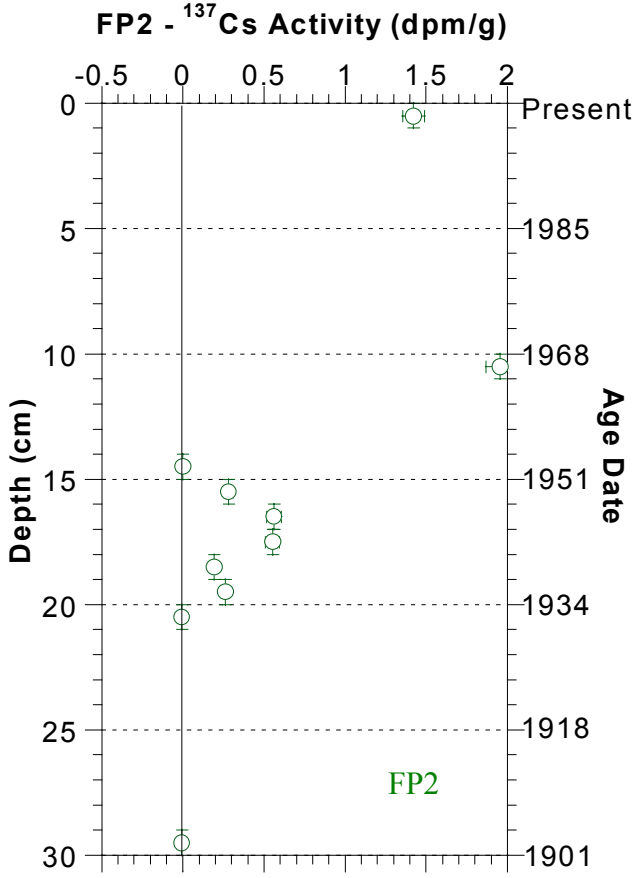

Figure 4-11. Measurements of ^{137}Cs activity for core FP2. Age dates are based on an estimated sedimentation rate from ^{210}Pb data of 3.0 mm/yr. Activity falls to 0 dpm/g at a depth of 20 cm.

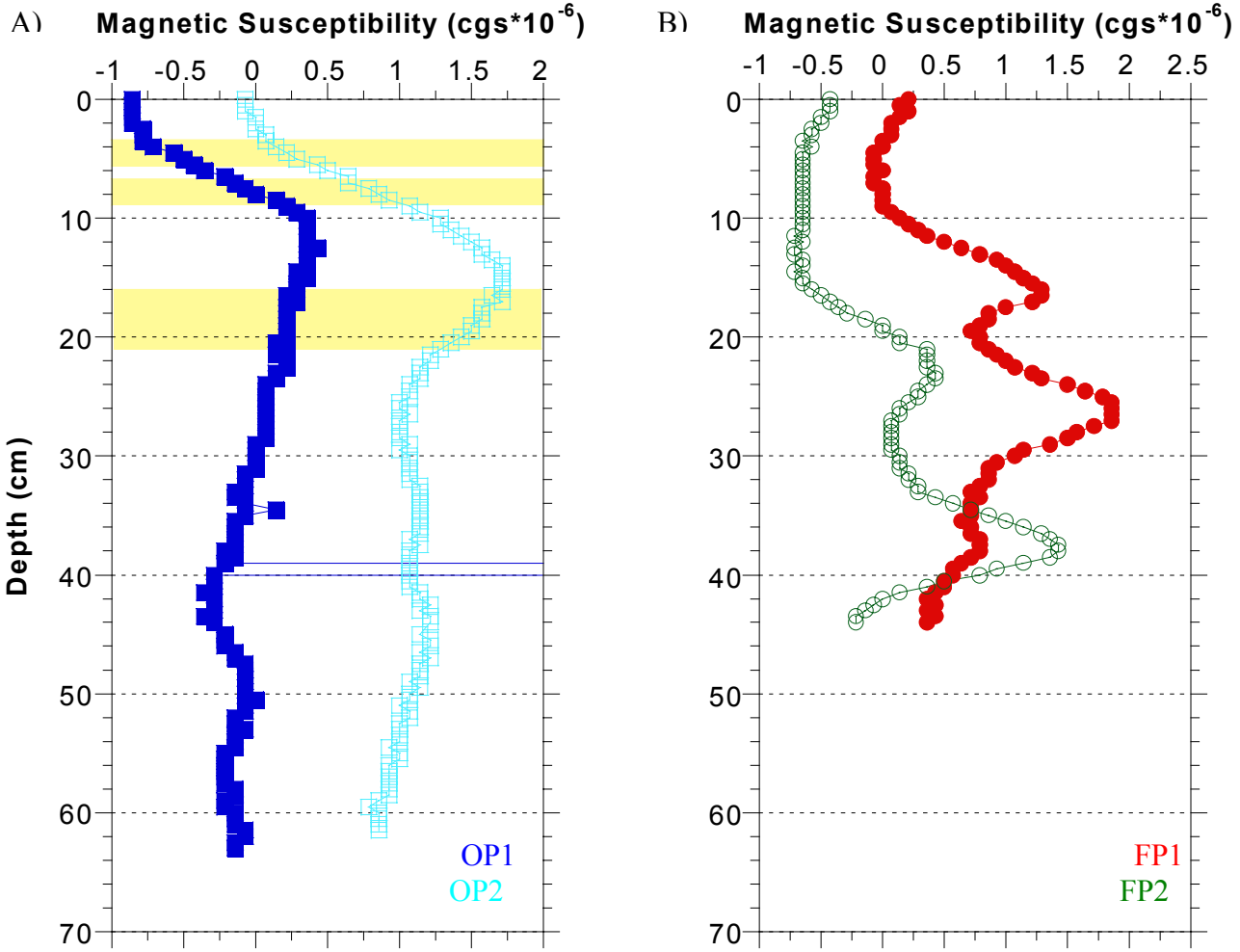

Figure 4-12. Magnetic susceptibility measurements for cores A) OP1 and OP2 and B) FP1 and FP2.

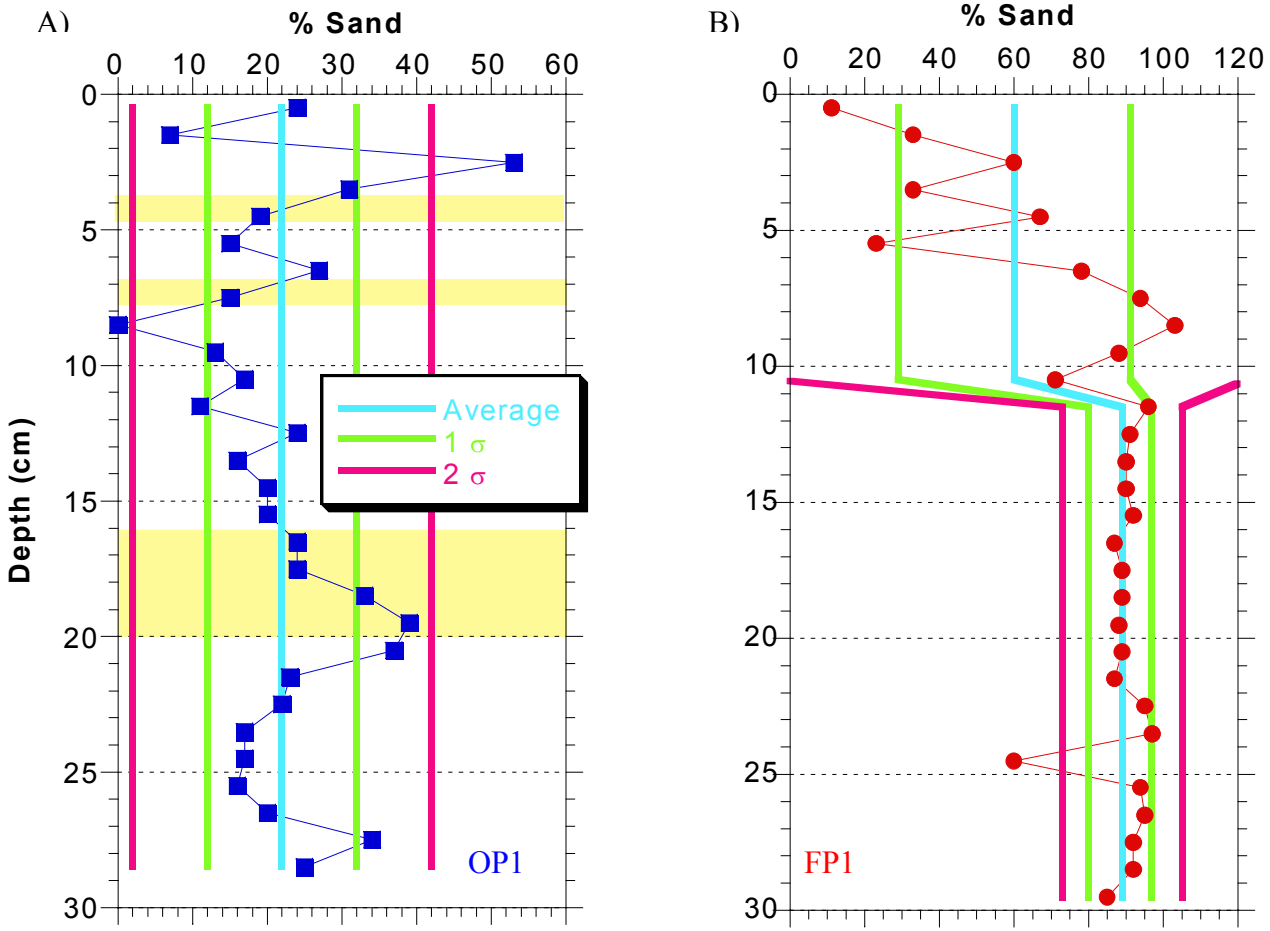

Figure 4-13. Percent sand data for cores A) OP1 and B) FP1. The light blue line represents the average for all samples for core OP1 and for samples from 0 to 10.5 cm and then 11.5 to 29.5 for core FP1. The green lines represent values that are one standard deviation from the mean and the pink lines represent values that are two standard deviations away from the mean. Yellow boxes represent depth matched to date of known hurricanes for OP1.

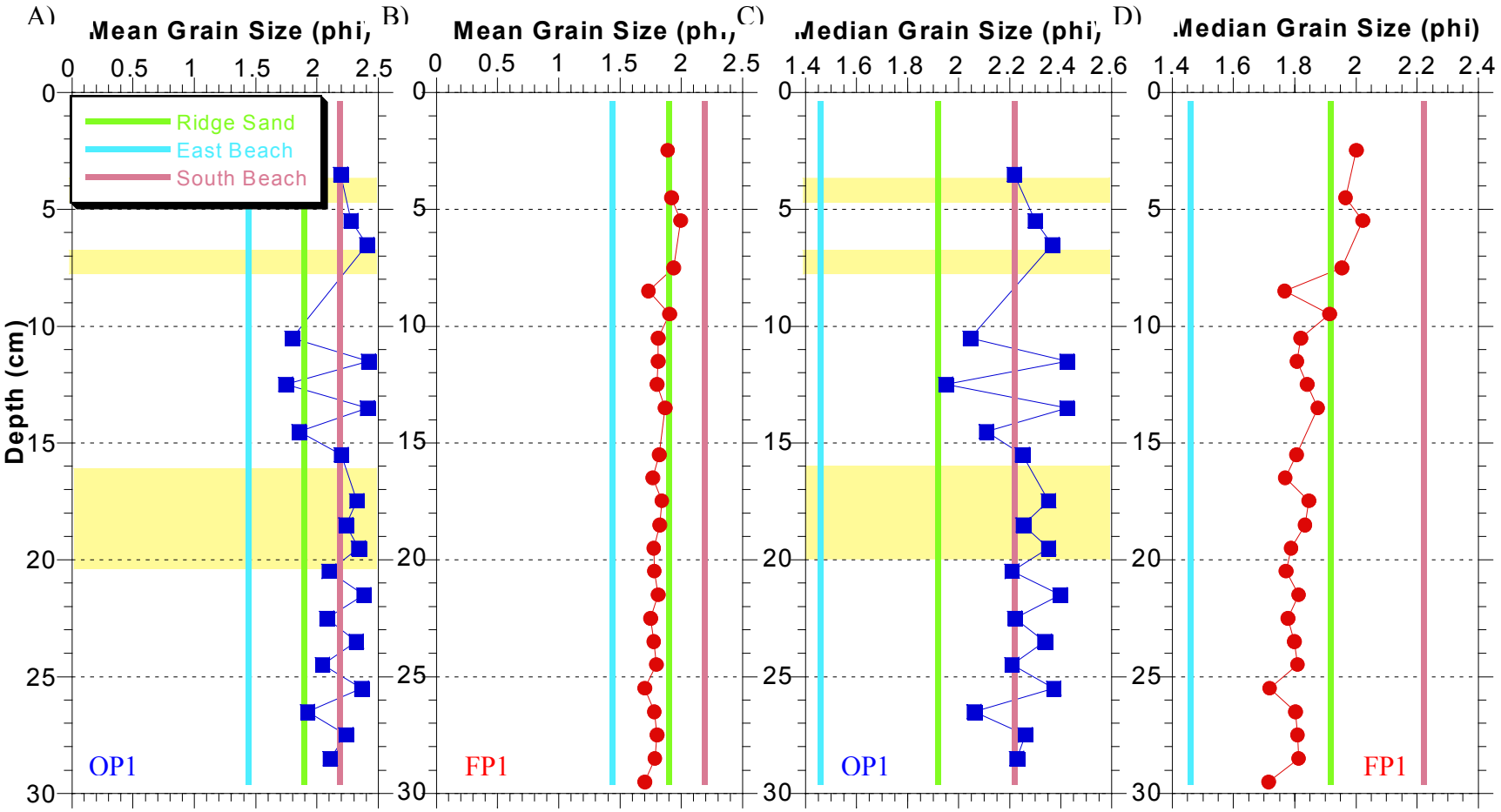

Figure 4-14. Mean grain sizes for cores A) OP1 and B) FP1 and median grain sizes for cores C) OP1 and D) FP1. Lines represent values for samples taken from the ridge sand, east beach, and south beach. Yellow boxes represent depth matched to date of known hurricanes for OP1.

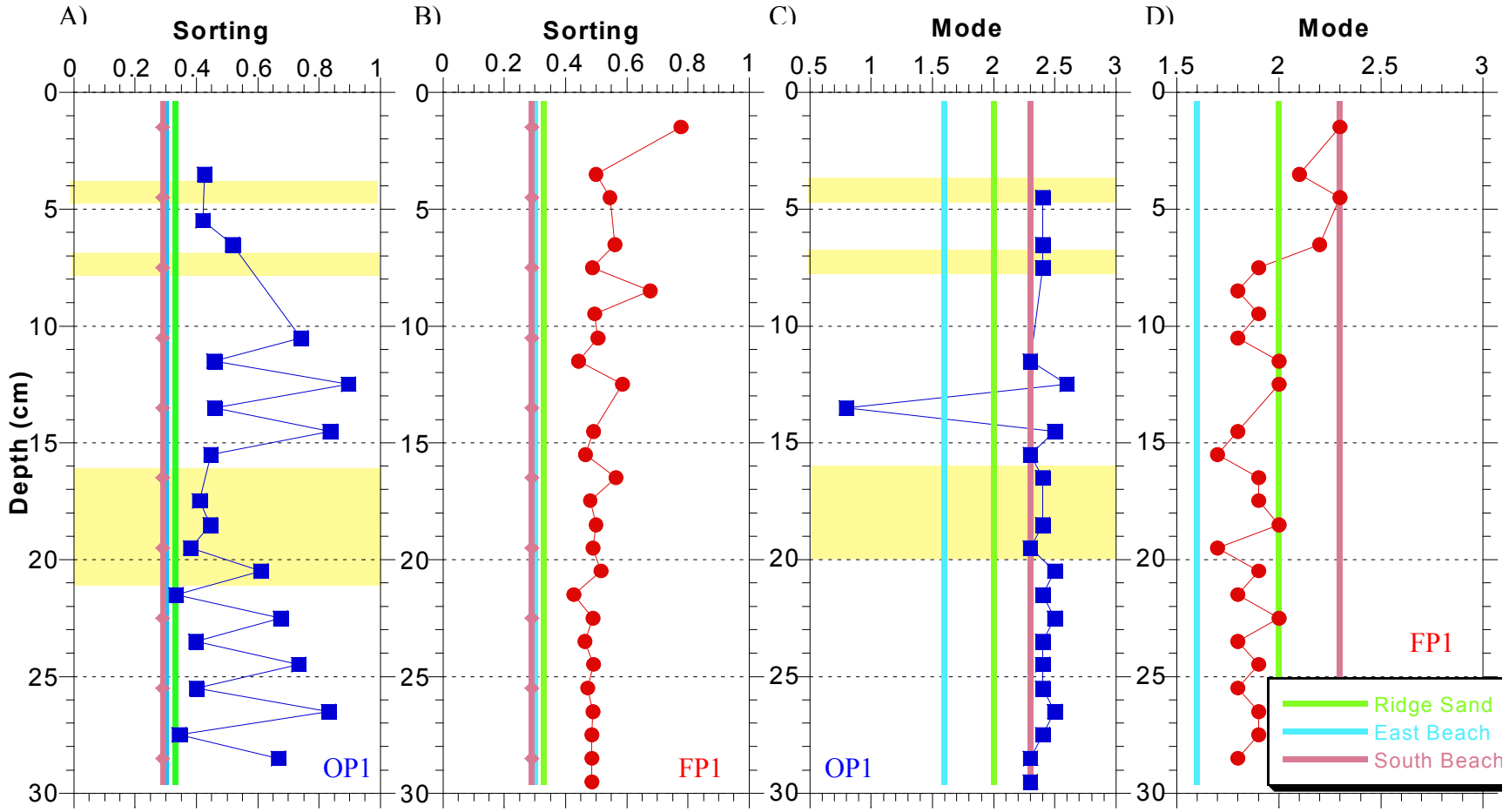

Figure 4-15. Sorting measurements for cores A) OP1 and B) FP1 and mode measurements for cores C) OP1 and D) FP1. Samples with sorting values less than 0.35Φ are very well sorted, 0.35-0.5 Φ are well sorted, 0.5-0.71Φ are moderately well sorted, 0.71-1 Φ are moderately sorted, 1-2 Φ are poorly sorted, and greater than 2Φ are very poorly sorted. Yellow boxes represent depth matched to date of known hurricanes for OP1.

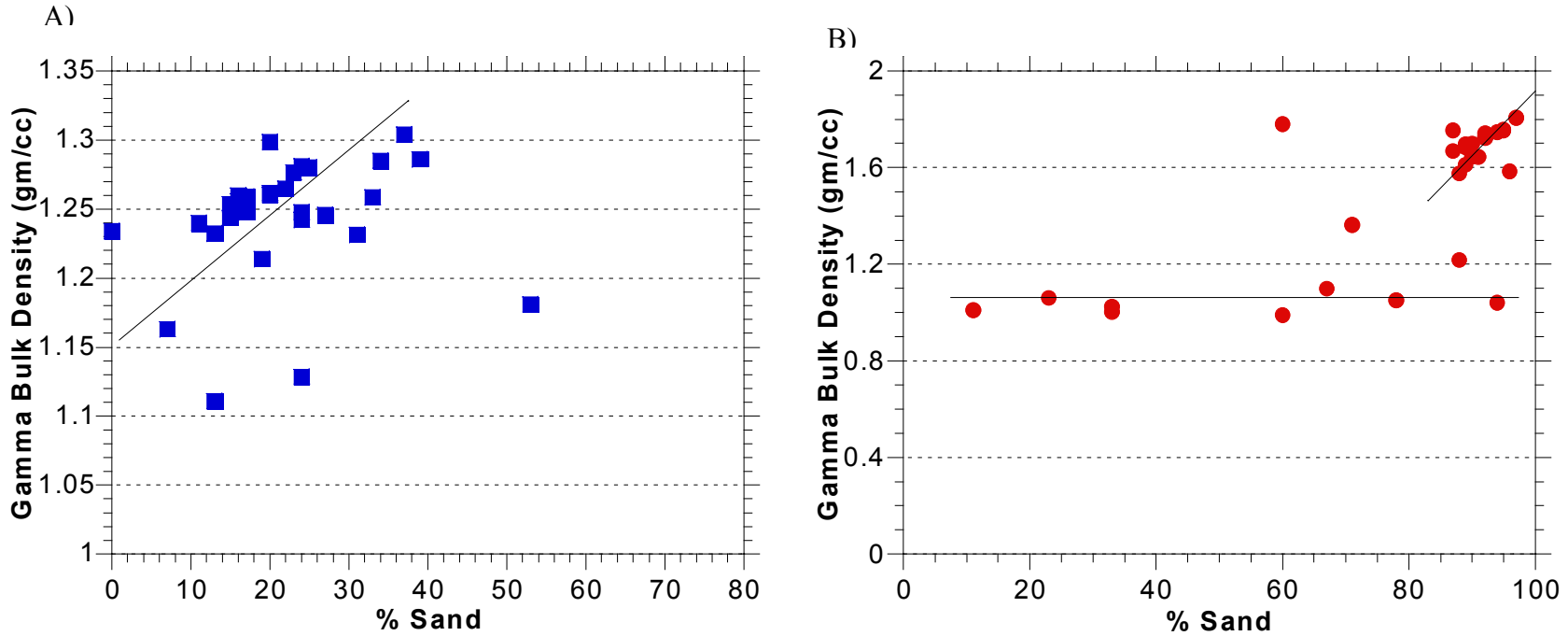

Figure 4-16. Plots of percent sand versus gamma bulk density (gm/cc) for cores A) OP1 and B) FP1. Black lines represent trends in the data.

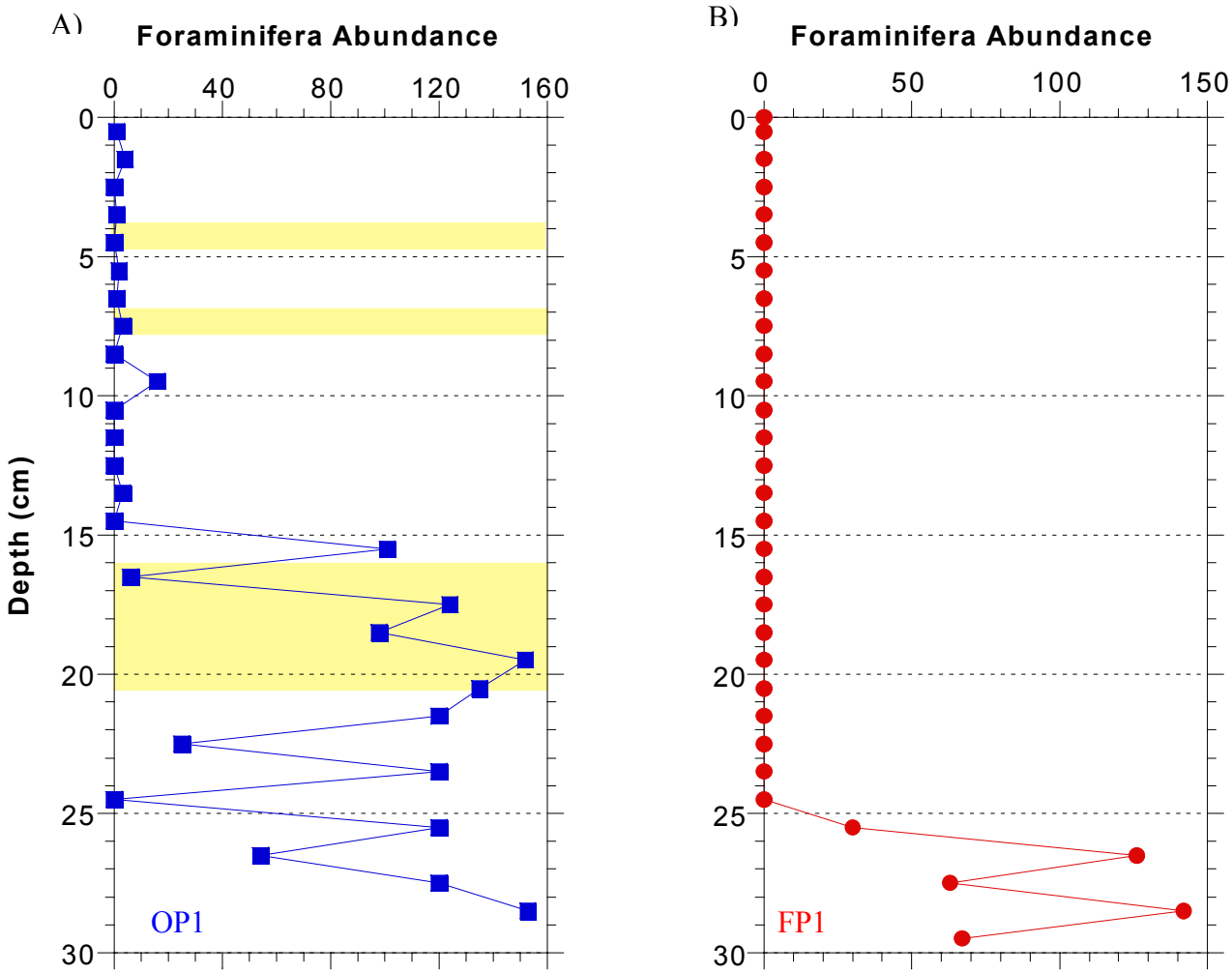

Figure 4-17. Foraminifera abundances per 0.3 g of sample for cores A) OP1 and B) FP1. Yellow boxes represent depth matched to date of known hurricanes for OP1.

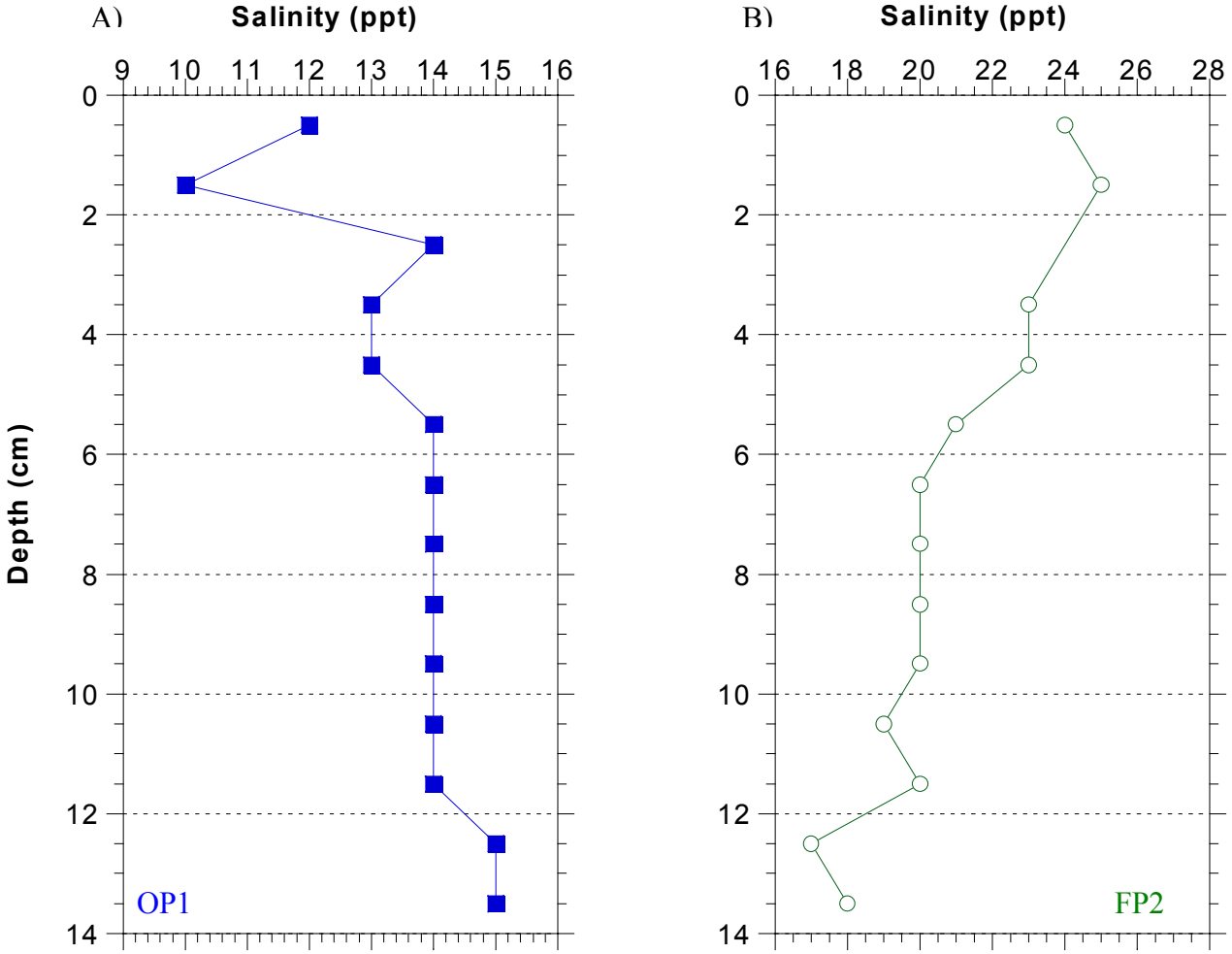

Figure 4-18. Salinity profiles for cores A) OP1 and B) FP2.

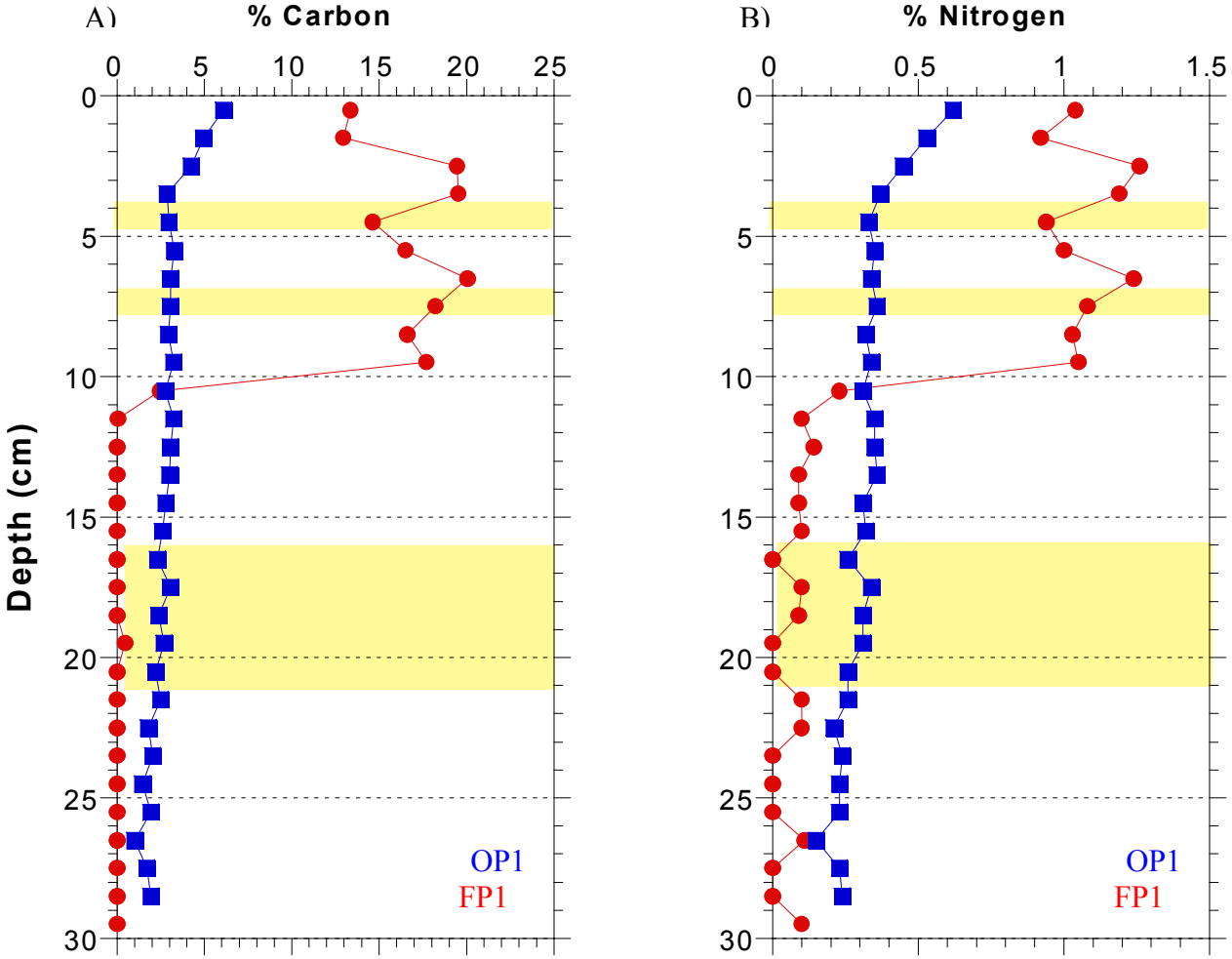

Figure 4-19. Percent organic carbon and nitrogen for cores A) OP1 and B) FP1.

CHAPTER 5
DISCUSSION

Geochronology

The constant rate of supply model (CRS) was used to calculate ^{210}Pb sediment accumulation rates (Appleby and Oldfield 1992). The model assumes that excess ^{210}Pb is delivered to the sediment at a constant rate. Consequently, as the bulk sedimentation rates increase, ^{210}Pb content in sediments is diluted and, conversely, as bulk sedimentation decreases, ^{210}Pb content is enriched (unless sediments are heavily bioturbated). The cumulative residual unsupported ^{210}Pb activity is calculated by Equation 5-1 (developed by Appleby and Oldfield 1992).

$$A_t = A_o e^{-kt} \quad (5\text{-}1)$$

where A_o is the cumulative residual unsupported ^{210}Pb (dpm/cm^2) below sediments of age t and k is the ^{210}Pb radioactive decay constant (0.03114 yr^{-1}) (Figure 5-1). The age of sediments (t) at depth x is calculated:

$$t_x = k^{-1}\ln(A_o A_x^{-1}) \quad (5\text{-}2)$$

where A_o is equal to the total integrated unsupported ^{210}Pb in the core and A_x is equal to the integrated activity of ^{210}Pb below depth x. The sediment accumulation rate is then calculated by dividing the dry weight of the sediment in the interval by the time represented by the interval (Figure 5-2).

Figures 4-8 and 4-9 show the unsupported, i.e. excess, and total ^{210}Pb activity profiles for cores OP1, FP1, and FP2. Core OP1 shows a decrease in activity with depth. In addition, measurements of ^{210}Pb activity for core OP1 reveal supported ^{210}Pb activity

at 18-19 cm. Therefore, this depth is approximated (within associated error) to be approximately 100 years old and gives an average sedimentation rate for the core of 1.8 mm/yr. Sediment accumulation rates calculated by the CRS model (using the dry bulk density of samples calculated as grams dry per cubic centimeters wet from freeze drying the samples) are between 0.1 and 7.8 mm/yr with an average of 3 mm/yr. These rates are much higher than the average estimated from excess ^{210}Pb first appearance and vary throughout the core.

Cores FP1 and FP2, on the other hand, contain alternating activity with depth, which complicates the use of the constant rate of supply model for calculating sediment accumulation rates because the depths with zero activity give accumulation rates of infinity (Appleby and Oldfield 1992). The average sedimentation rates for these cores can be estimated by the depth of excess ^{210}Pb first appearance. For core FP1 this depth is at ~15 cm, giving an average sedimentation rate of 1.5 mm/yr. Core FP2 appears to reach a ^{210}Pb activity of 0 dpm/g at 30 cm for an average sedimentation rate of 3.0 mm/yr. Samples were not measured for ^{210}Pb below this depth, so it is not possible to say for sure that this is the depth of first appearance.

Activity for ^{210}Pb is commonly reported as inventory (dpm/cm^2). The plot of ^{210}Pb inventory for core OP1 (Figure 5-1) shows similar trends to the plots of total and excess ^{210}Pb activity (dpm/g) (Figure 4-8) with the exception of core FP1 at depths of 11, 13, and 15 cm. Data for these samples plot higher than when reported as dpm/cm^2. The difference is due to the higher sand content and, therefore, greater mass of samples downcore.

All dates given for core FP1 in Figure 4-8 and FP2 in Figure 4-9 use the sedimentation rates estimated from the first appearance of ^{210}Pb activity. The higher sand content of Flag Pond is the proposed reason for the sporadic ^{210}Pb activity profile, as sands have less surface area for radioisotope adsorption. Dating using ^{210}Pb works best if used in fine grained, highly organic sediments (Appleby and Oldfield 1983, Collins et al. 1999, and Schelske et al. 1994).

Concentrations of ^{137}Cs were used as another means of dating the cores. The method assumes first appearance of ^{137}Cs occurred ~1954. The radioisotope was introduced into the atmosphere beginning in 1954, from atmospheric atomic weapons testing (Smith and Comans 1996). ^{137}Cs profiles are also influenced by depositional diffusion because it is more mobile in sediments than ^{210}Pb. The first appearance for ^{137}Cs in core OP1 occurs at a depth of 12 cm (Figure 4-10), which agrees well with the age calculated by the ^{210}Pb method. The ^{137}Cs profiles of cores FP1 and FP2 (Figures 4-10 and 4-11), like the ^{210}Pb profiles, were irregular, but depths for the first appearance of ^{137}Cs activity could be estimated. Core FP1 first showed ^{137}Cs activity at 11.5 cm, while core FP2 showed activity at 19.5 cm. Although these depths do not correspond with the depths calculated to be 1954 based on the sedimentation rates approximated from ^{210}Pb activity (which are ~7 cm for core FP1 and ~14 cm for core FP2), a chronology can be estimated for core FP2. According to the ^{137}Cs activity data, sediments at 20 cm depth for core FP2 are estimated to correspond to ~1950. All sediment above this depth is younger than 1950. Sediments at 30 cm depth correspond to ~1880-1900 according to the first appearance of excess ^{210}Pb activity. The dates calculated by ^{137}Cs and ^{210}Pb activity give sediment accumulation rates ranging from ~3.8 mm/yr for sediments above

20 cm to ~3.0 mm/yr for sediments below 30 cm. A rather limited range of accumulation rates for core FP2 is possibly due to uneven sedimentation. Storm events could have deposited one or more thick beds of sand at some point after 1950 and increased the sediment accumulation rate for a brief period. Storm activity would also account for the variability in the sedimentation rate seen in core FP1 (Figure 5-2). Increases in wind-blown material into the ponds may also temporarily raise sedimentation rates for both of the Flag Pond cores.

In order to determine if there is migration of ^{137}Cs within the cores, the Peclèt (Pe) number, a scaling argument between advection and diffusion, was calculated for cores OP1, FP1, and FP2 using the following equation (Boudreau 1997):

$$Pe = [(1+K_d)*S*L]/D_s$$

where K_d is the solid-liquid distribution coefficient (10^2-10^3), S is the sedimentation rate (cm/yr), L is the length of the scale of interest (5-10 cm), and D_s is the sediment diffusion coefficient for ^{137}Cs (~500 cm^2/yr) (Sugai et al. 1994). The K_d value is based on values reported for lakes by Sugai et al. (1994). If the Pe>>1, then ^{137}Cs diffusion is negligible. Tables 5-1 through 5-4 shows the results for the above calculations.

Table 5-1. Results for the calculation of the Peclet number for cores OP1, FP1, and FP2 for a K_d value of 10^2 and an L value of 10 cm For Pe>>1, diffusion of ^{137}Cs is negligible.

Core	OP1	FP1	FP2
K_d	10^2	10^2	10^2
S (cm/y)	0.18	0.15	0.30
L (cm)	10	10	10
D_s (cm^2/y)	500	500	500
Pe	0.36	0.3	0.6

Table 5-2. Results for the calculation of the Peclet number for cores OP1, FP1, and FP2 for a K_d value of 10^5 and an L value of 10 cm. For Pe>>1, diffusion of ^{137}Cs is negligible.

Core	OP1	FP1	FP2
K_d	10^3	10^3	10^3
S (cm/y)	0.18	0.15	0.30
L (cm)	10	10	10
D_s (cm^2/y)	500	500	500
Pe	3.6	3	6

Table 5-3. Results for the calculation of the Peclet number for cores OP1, FP1, and FP2 for a K_d value of 10^2 and an L value of 5 cm. For Pe>>1, diffusion of ^{137}Cs is negligible.

Core	OP1	FP1	FP2
K_d	10^2	10^2	10^2
S (cm/y)	0.18	0.15	0.30
L (cm)	5	5	5
D_s (cm^2/y)	500	500	500
Pe	0.18	0.15	0.3

Table 5-4. Results for the calculation of the Peclet number for cores OP1, FP1, and FP2 for a K_d value of 10^5 and an L value of 5 cm. For Pe>>1, diffusion of ^{137}Cs is negligible.

Core	OP1	FP1	FP2
K_d	10^3	10^3	10^3
S (cm/y)	0.18	0.15	0.30
L (cm)	5	5	5
D_s (cm^2/y)	500	500	500
Pe	1.8	1.5	3

The calculated Peclet numbers show that diffusion of ^{137}Cs is influencing the activity profile, and thus the first appearance, when the solid-liquid distribution coefficient is 10^2. When the coefficient is slightly larger (10^3), there is a balance between diffusion and advection over 5-10 cm. The length of scale does not appear to affect the results of the calculation.

According to ^{210}Pb data, the predicted depth that corresponds to 1954 (the estimated date for the first appearance of ^{137}Cs) is 13 cm for core OP1 and 7 cm for core FP1. The ^{137}Cs activity data shows a first appearance at 12 cm for both of these cores,

indicating that the diffusion of ^{137}Cs is as much as 9 and 69%. The difference in the sediment accumulation rates calculated for the two radioisotopes is 0.02 cm/yr for core OP1 and 0.9 cm/yr for core FP1.

Mass sediment accumulation rates vary with depth in core OP1 (Figure 5-2). The highest sediment accumulation rates (150-200 mg/cm^2/yr) are seen at depths of 8.5, 9.5, and 11.5 cm, but the increases are only 30-50 mg/cm^2/yr (30-35%) greater than other depths. It is hypothesized that a hurricane would bring in increased amount of material and, therefore, increase sedimentation rates (as mentioned above). The depths of the increased sediment accumulation in core OP1 do not match with any known hurricanes. Error associated with ^{210}Pb age dating is one possible cause for the offsets.

The sediment accumulation rates for core FP1 (Figure 5-2) are much higher than for core OP1. Three spurious samples (at 1.5, 3.5, and 13.5 cm) reach accumulation rates greater than 4000 mg/cm^2/yr and another sample (at 8.5 cm) has an accumulation rate of 2622 mg/cm^2/yr. All other samples for this core vary between 36 and 795 mg/cm^2/yr. The sediment accumulation rates were calculated by the CRS model and may not be accurate due to the irregularities of the ^{210}Pb activity profile. The model calculates accumulation rates of infinity for depths with zero or near zero ^{210}Pb activity.

The sedimentation rates for the coastal ponds on St. Vincent Island (1.5-3.0 mm/yr) are on the low end of the rates reported for other coastal ponds (Table 5-5). The sedimentation rate is comparable to the rates reported by Liu and Fearn (1993) (0.3-4.5 mm/yr) for Lake Shelby in Alabama and Donnelly et al. (2001a) (2-2.5 mm/yr) for Succotash Marsh in Rhode Island. Accumulation rates are likely low in general for Oyster and Flag Ponds due to the low elevation and the small drainage basin of the

island, which prevent increased amounts of sediment from entering the ponds (St. Vincent National Wildlife Refuge, Apalachicola, Fl., 2000, Final Report of the Vegetation Survey and Map Project, A USFWS-USGS Research Partnership Program Project).

Table 5-5. Sedimentation and mixing rates for several coastal ponds.

Location, Reference	Sedimentation Rates (mm/yr)	Method Used	Mixing Rates (cm^2/yr)	Method
Texas Estuary (Ravichandran et al. 1995)	4--5	^{239,240} Pu	0.04-0.4	^{239,240} Pu
Maine Coastal Pond (Norton et al. 1997)	0.15	^{210}Pb	N/A	N/A
Texas Tidal Lake (Williams 1995)	1--45	^{210}Pb, ^{137}Cs	Mentioned, not quantified	N/A
KwaZulu-Natal Coastal Lake (Scott and Steenkamp 1996)	1.5-5.5	Radiocarbon	N/A	N/A
England Coastal Lake (O'Sullivan et al. 1991)	9	^{210}Pb	Mentioned, not quantified	N/A
St. Vincent Island, Florida	1.5-1.8	^{210}Pb,^{137}Cs		

There are limitations on establishing a robust and high resolution chronology for the cores from St. Vincent Island. The high sand content of the Flag Pond cores prevents a reliable ^{210}Pb activity profile because the lead particles do not adsorb to sand as readily as organic matter. The measured activity is equal to the activity adsorbed times the mass flux. If all particles do not adsorb to the sand or if there is variable adsorption, then measurements of activity do not accurately reflect the initial concentration of ^{210}Pb and, therefore, cause discrepancies in decay calculations. Consequently, sedimentation rates for cores FP1 and FP2 can only be estimated based on the first appearance of ^{210}Pb and ^{137}Cs activity. Core OP1 fits logarithmic isotope profiles for ^{210}Pb and ^{137}Cs activity, but the errors associated with excess ^{210}Pb activity are quite high (up to 1.2 dpm/g). These

limitations make it difficult to correlate the age of known hurricanes to the approximate depth at which they occur. Due to the error associated with the age-depth relationships, it is difficult to relate the proxy records to individual hurricanes.

Signal

Coastal environments are very dynamic and it is often difficult to observe the paleocyclone signal within such a dynamic depositional environment. It is best to study preservation of paleostorm bedding where the signal is strongest. Subtidal environments are constantly altered due to biological, wave, current and tide activity, resulting in rapid post-depositional mixing after event bed deposition (Wheatcroft and Drake in press). Supratidal environments offer the best paleostorm record because there is little physical activity within the environment from waves and currents and inundation from tides only occurs during intense storms. Tropical cyclones making landfall, therefore, should generate enough energy to transport both water and sediment from offshore and deposit them in the supratidal environment as overwash and aeolian deposits (Collins et al. 1999, Liu and Fearn 2000).

Based on previous studies, storm event layers are hypothesized to have a coarser mean grain size and be more poorly sorted than *insitu* sediments (Davis et al. 1989, Liu and Fearn 2000, Donnelly et al. 2001). Although the mean and median size of the sand fraction for core OP1 shows some variations (Figure 4-14), they are on a very small scale (<1 phi difference) and there are no pronounced intervals (+1 σ) that stick out from the rest of the data as representing an event (Wheatcroft and Drake in press). The interval from 10-15 cm shows increased variations that may be associated with a storm deposit, but this interval does not correlate to any of the depths associated with known hurricanes. Although there is abundant vegetation separating Oyster Pond from the south beach, the

mean size of the sand fraction for this core plots very closely with the mean grain size of the south beach. Almost all of the samples from Oyster Pond are greater than 2Φ in size. Currents of 25 cm/s are required to move grains this large (Prothero and Schwab 1996). Because velocity is inversely related to shear stress and equal to the volume times the cross sectional area, sediment brought in as overwash would drop out of suspension very quickly after crossing over the dunes and into the ponds and deposit very near the shoreline closest to the beachface. Thus, the sand is most likely brought into Oyster pond on a semi-regular basis as aeolian deposits during strong storms with winds greater than 25 cm/s.

Core FP1 (Figure 4-14) shows very little variation (<0.2 phi) in mean and median size of the sand fraction. The data plot very close to that of the ridge sands, which implies that the sand is derived from inland or Flag Pond is a submerged part of the ridge system making up the island. The grain size for this pond appears to be influenced more by its surrounding environment than by aeolian material from the south beach despite its closer proximity to the beach than Oyster Pond. Also, the vegetation surrounding Flag Pond is dense and may prevent transfer of some sediment by the wind.

The sorting of the sand fraction for samples from core OP1 (Figure 4-15) does show some layers to be more poorly sorted (10-15 cm and 20-29 cm). Within the error associated with dating, it is possible that the sorting profile shows some evidence of hurricane deposits. Core FP1 shows a fairly continuous sorting profile downcore for the sand fraction with no indication of event layers. No other previous paleocyclone studies document specific data regarding grain size and sorting, other than to say that storm deposits had higher sand content and were poorly sorted. Parsons (1998) reported that

the deposit left by Hurricane Andrew showed a coarser grain size, but did not have the graded profile discussed by Davis et al. (1989). He suggested that the sampling interval (0.5 cm) may have been too large to show any grading associated with the deposit. Because this sampling interval is smaller than that used for the samples from St. Vincent Island (1 cm), it could also be the reason for the lack of distinct layers of coarse grain size and poor sorting. Liu and Fearn (1993) also report storm deposits on the millimeter scale that were identified visually.

The sorting profiles for both ponds plot higher than all three environments sampled on the island, implying that the ponds are more poorly sorted than any single environment and are receiving a mixture of material from different environments. Modal values, similar to mean and median values, for core OP1, plot very closely with the south beach and have an outlier point at 13.5 cm. The modal profile for core FP1 plots closely to the ridge sands below 7.5 cm and then trends toward the south beach upcore indicating a shift in source material. The shift in modal values corresponds to a shift in values for percent sand, implying that increased amounts of sand began entering Flag Pond from a new source.

The percent sand is expected to increase for a storm bed as more sand is brought in as wind-blown material into muddier ponds (Donnelly et al. 2001). There are some very noticeable increases in percent sand (at 2 cm to 53%, 6 cm to 28%, and 20 cm to 40%) for core OP1 that are slightly offset from the depths that match known hurricanes (Figure 4-13). However, the offsets are within 2 cm and could be related to sampling and/or dating error. The samples that did not fit the trendline when percent sand was plotted against gamma bulk density (Figure 4-16) are most likely related to consolidation effects

after sampling. The increases in percent sand for core FP1 (Figure 4-13) could correlate with the 1974-75 (60% sand at 2 cm) and 1985 (65% sand at 4 cm) hurricanes. Because of dating problems with the Flag Pond cores, there is no way to establish an accurate age-depth relationships relating proxy records of hurricanes.

Decreases in percent organic carbon and percent nitrogen are hypothesized to correspond to coarse sediment layers that may be associated with hurricane deposits (Parsons 1998). Figure 5-3 shows that although trends do exist when percent sand is plotted against percent organic carbon, there is no evidence that increases in percent sand correspond to decreases in percent organic carbon. Core OP1 shows similar trends with respect to percent organic carbon and nitrogen (Figure 4-19). The exponential decrease in core OP1 in both values argues for strong diagenetic decomposition that would mask any episodic increases. Core OP1 does not have any increases or decreases in percent organic carbon or nitrogen that could be hurricane related. Although core FP1 shows trends very different from core OP1, there are similarities in trends between percent organic carbon and percent nitrogen (Figure 4-19). Core FP1 has small (3-4 %) decreases in both proxies that could correlate to the 1974-75 and 1985 hurricanes. In general, the decreases in percent carbon seen in core FP1 at 4.5 and 8.5 cm are minor compared to the decreases documented by Collins et al. (1999) for the core taken at the location directly impacted by Hurricane Hugo (from >20% to 0.6-3%) and show a large decrease in organic carbon due to the low content of organic carbon in beach sand. However, in the core taken 50-75 km away from the location of landfall of Hurricane Hugo, there were no noticeable decreases in percent carbon implying a lack of deposition of a storm bed at this distal site. Parsons (1998) also reported that percent carbon showed

decreases throughout cores taken in a Louisiana marsh, but that this proxy was not a useful indicator of storm layers due to the diagenetic control of carbon decomposition.

The rapid increase in organic carbon accumulation could be related to a change in the environment of the pond. Prior to the mid-1900's the area that is now submerged may have been a dry, sandy low point between beach ridges. A large storm could have hit the island with winds strong enough to move sand around and create an enclosed area within the low point of the beach ridges. Water level increases in the enclosed area could have allowed for the establishment of aquatic vegetation, thereby increasing the percent of organic carbon in the sediments. Due to difficulties associated with ^{210}Pb dating, it is not possible to correlate the formation of the pond with any specific storm. Although the transition from sand to organic rich sediments does not occur at the same depth for both of the Flag Pond cores (at ~10 cm for FP1 and ~20 cm for FP2) (Figure 4-1), the age dates calculated for both cores match within the associated dating error (Figures 4-8 and 4-9).

The foraminifera abundances (Figure 4-17) were measured because it was hypothesized that marine forams would be transported into the predominantly freshwater and brackish ponds by storm surge during cyclones. Greater than 90% of the foraminifera belonged to the genus *Ammonia*, which is characteristic of detrital-rich environments such as continental shelves and lagoons. This species is known to exist in a wide variety of environments from brackish and hypersaline waters to freshwater, as such, *Ammonia* are able to exist under very stressful conditions. In addition, there is a noticeable absence of *Miliolidae* and *Elphidium*, which are common to shallow, nearshore and marsh sediments in Florida (Rose and Lidz 1977). This is a contrast to the

findings of Collins et al. (1999), where they observed that even in cores taken at 50-75 km from where Hurricane Hugo came ashore, offshore species of foraminifera were abundant at depths dated to the time of the hurricane landfall. The cores from South Carolina showed no other sedimentological evidence for hurricane landfall other than the presence of offshore foraminifera.

While foraminifera have been useful in other paleohurricane studies (Collins *et al*. 1999), there are no foraminifera in samples above 15 cm for core OP1 and 25 cm for core FP1. Therefore, the foraminifera data cannot be used as a proxy for hurricane activity at this site. The conditions in the pond may no longer be suitable for the foraminifera to survive, although this is unlikely given the ability of *Ammonia* to tolerate very stressful conditions. Rather, an increase in organic matter to the sediments could have caused an increase in organic carbon decomposition, which would increase CO_2 production in sediment porewaters. Increases in CO_2 lower pH, leading to abundant calcite dissolution and loss of fossil record (Green et al. 2001).

Magnetic susceptibility (Figure 4-12) was used as a proxy for storm deposits because increases in magnetic susceptibility may reflect changes in sediment provenance. Magnetic susceptibility measures whether minerals are diamagnetic (biogenic carbonate and silica) or paramagnetic (Fe-rich silicates including clays). Diamagnetic minerals have a negative magnetic susceptibility, while paramagnetic minerals are positive (Frederichs et al. 1999). There appear to be clear intervals of increased (positive) magnetic susceptibility, which indicate intervals with more Fe-rich silicates. Such increases in magnetic susceptible minerals may reflect periodic input of heavy mineral sands to the ponds, although the increases are small and may reflect very minor additions

of such minerals. Both cores from each respective pond correlate well to each other, with common patterns in layers of positive magnetic susceptibility reflecting a common source. The increases in magnetic susceptibility at 14-16 cm for core FP2 and at 38 cm for core OP2 match with increases in gamma bulk density. The offset of the peaks for cores FP1 and FP2 is most likely related to the difference in the estimated sediment accumulation rates. However, these layers do not seem to correlate to the depths of known hurricanes. The loop used to test the cores integrates over a range of 10 cm (Weber et al. 1997), which is far too coarse a sample interval (~20 years) to detect individual storm beds that may be only one mm thick. Also, inflection points may be due to dilution from diamagnetic silica. No other studies have used magnetic susceptibility as a proxy for hurricane deposits.

The gamma bulk density (Figures 4-2 and 4-3) shows some correlation to known hurricanes for the Oyster Pond cores, but because the sampling interval is 0.5 cm, it is difficult to correlate with other variables sampled at coarser resolution. Core OP1 shows a peak in the 17-22 cm range that may correlate with the 1886 hurricane, whereas core OP2 has peaks in bulk density at 8-9 cm and 16-19 cm that may relate to the 1974-1975 and 1886 hurricanes using a chronology that is approximated from that of core OP1. The Flag Pond (Figure 4-5) cores do not show any peaks that relate to known hurricanes. The large increases in bulk density (at 12 cm for core FP1 and 36 cm for core FP2) are likely related to the environmental shift mentioned above in relation to organic carbon. Difficulties establishing age-depth relationships make correlations difficult. Bulk density could correlate well with percent sand if there were no compaction or bioturbation. Figure 4-16 shows a potential relationship between bulk density and percent sand for core

OP1. The two separate trends for core FP1 in Figure 4-16 indicate a consolidation due to the change in lithology. Because percent sand and bulk density correlate well, it may be necessary to measure one of these parameters in paleocyclone studies. Bulk density was not used as a parameter for identifying paleostorm deposits in previous studies.

The x-radiographs (Figure 4-6) show greater detail of bedding, changes in lithology, and bioturbation than the photographs. Bedding changes, changes in density, and worm tubes that are beneath the surface are visible in the x-radiographs. They reveal that some of the bedding is slanted across the core, while other beds are parallel across the core. The subsampling of the cores was done perpendicular to the core wall and would have, thus, cut across these slanted beds and, therefore, prevented samples for other proxy records from fully representing event layers. The x-radiographs also reveal information about the depth of biologic activity. Worm tubes (<0.5 cm in diameter) extend down to a depth of 3 cm in core OP1 and 2 cm in core FP1.

In addition to visual examination of sedimentary structures, the x-radiograph pixel density data are the proxy record that resolves a strong signal for paleocyclones (Figure 4-6). Pixel density (0-255 gray scale) is controlled by the absorption of x-rays by the film and variability in pixel intensity roughly corresponds to the bulk density of the sediments. The x-radiographs were sampled at high resolution (~1 mm) and can detect layers that are thinner than the 0.5 cm layers measured for gamma bulk density. Both of the Flag Pond cores show increases in pixel density that may correlate to the 1985 and 1974-75 hurricanes (40 pixel density increases at 3 and 5 cm), but difficulties with the Flag Pond chronology prevent an exact correlation. Core FP1 may also show evidence of the 1886 hurricane, but the increase is masked by the increase related to the

environmental shift mentioned above. The Oyster Pond cores show several increases in pixel density (at 14, 31, and 36 for core OP1 and at 8, 24, and 29 for core OP2), but they are offset from the depths corresponding to the dates of hurricanes, possibly due to dating errors. Both cores have increases (at 19 cm for core OP1 and 17 cm for core OP2) that correspond to the depth of the 1886 hurricane. The chronology for core OP2 is estimated by correlation with OP1. Due to its high-resolution sampling, the pixel density shows a detailed record of event layers that supports the percent sand data. Increases in both proxies are seen at 2.5, 6.5, and 19.5 cm for core OP1 and at 2.5, 4.5, and 23.5 for core FP1.

The salinity data for core OP1 (Figure 4-18) have an irregular profile above 4 cm and then remain between 13 and 15 ppt downcore. Core FP2 trends from saline to fresher water with increasing depth. The trend suggests that the pond was previously either a fresh marsh or influenced by fresh groundwater and that the saltwater has not fully diffused through the sediments. Also, the pond may still experience freshwater intrusion from the groundwater and saltwater spray from the ocean and the trend reflects a mixture of the two sources.

Table 5-6 is a summary of all of the proxies tested and whether they showed any evidence of the 1886, 1974-75, and 1985 hurricanes. Due to the uncertainties associated with the dating of the Flag Pond cores, it is impossible to match proxy records to specific hurricanes. All data in Table 5-6 only relate to the Oyster Pond cores. There are large errors associated with the dates calculated for core OP1, which also make it difficult to match specific hurricanes. The 1886 hurricane appeared to be detected the most frequently. The 1974-75 hurricanes appeared to be recorded by two of the proxies tested.

The more recent 1985 hurricane appeared to be evident in three of the proxy records. Because of the increased error associated with the 1886 date, the range of possible depths that could correspond with the date of this hurricane is quite large allowing for a greater number of proxy records to fit within this range.

Table 5-6. Synopsis of detection of hurricanes by each of the proxies tested. The 1886 hurricane was a category five. Hurricane Carmen (Category 3) occurred in 1974 with Hurricane Eloise (Category 3) followed in 1975. Hurricanes Elena (Category 3) and Kate (Category 2) and Tropical Storm Juan all occurred in 1985.

Proxies	1886	1974-75	1985
Visual Examination	No	No	No
Gamma Bulk Density	Yes	Yes	Yes
Pixel Density	Yes	Yes	Yes
Sediment Accumulation Rates	No	No	No
Magnetic Susceptibility	No	No	No
Percent Sand	Yes	No	Yes
Mean Grain Size of Sand	No	No	No
Median Grain Size of Sand	No	No	No
Sorting of Sand Fraction	Yes	No	No
Mode Grain Size of Sand	No	No	No
Foram Abundance	No	No	No
Salinity	No	No	No
% Carbon	No	No	No
% Nitrogen	No	No	No

Preservation Potential

It is important to determine preservation potential of coastal depositional environments when studying paleocyclone deposits because a combination of strong sediment mixing and low sedimentation rates may make it difficult to preserve deposited cyclone deposits. If coastal sedimentary strata do not show any evidence of past hurricane activity, then a low preservation potential for that area could be one explanation. If that same environment has a high preservation potential, but lacks a

strong sedimentological signal, then it is likely that that no bedding from hurricanes has been deposited during the time period that the strata represent.

The preservation potential of an event layer (Figure 5-4 and 5-5) can be estimated from comparing transit time (the time required for an event layer to travel through the surface mixed layer) to dissipation time (the time required for an event deposit to be completely destroyed). Transit time is calculated by the equation developed by Wheatcroft and Drake (in press):

$[(L_b-L_s)/2]$/Burial Rate = Transit time of event layer

where L_b is the thickness of the surface mixed layer and L_s is the thickness of the event layer. L_b incorporates both physical and biologic mixing. The units for both L_b and L_s are centimeters, while burial rate is recorded as cm/yr and preservation potential is calculated as a percentage of the original signal. The thickness of the event bed represents the sediment transport potential of the storm and is a function of available sediment for transport, shoreline vegetation, dune morphology, distance of coastal pond from shore, and storm surge. Storm surge is related to the forward speed of the storm, amount of rainfall, wind speed, and duration of storm (Davis et al. 1989 and Risi 1998). Other hurricane studies report event bed thickness ranging from 0.1 to 30 cm (Liu and Fearn 1993 and 2000, Donnelly et al. 2001a,b, Davis et al. 1989, and Collins et al. 1999). However, Liu and Fearn (1993) do not detail how they were able to detect event layers that were 0.1 cm thick, nor why these beds were preserved.

In order for an event layer to be well preserved, transit time must be greater than dissipation time. Therefore, L_s needs to be much greater than L_b. Figure 5-4 demonstrates that when L_b is thicker than L_s, the event layer is mixed by biologic and

physical mixing but remains detectable. When L_s is greater than L_b, the upper part of the event layer is mixed, but preserved further down as it is below the depth of mixing (Figure 5-5).

For St. Vincent Island, the thickness of the surface mixed layer was calculated based on ^{210}Pb profiles and x-radiographs. If surface sediments have been rapidly mixed, the ^{210}Pb profile may have a near-surface interval of constant activity before exponentially decreasing (Figure 5-6) (Sugai et al. 1994). Core OP1 did not have such an interval, but did show evidence for mixing in its x-radiographs, as worm tubes extend down 1-2 cm from the surface, depending on the core. ^{210}Pb data for core FP1 were not reliable for determining mixing depth. The x-radiographs for this core also show worm tubes down 1-2 cm from the surface. Taking all of these factors into consideration, the rapidly mixed L_b for St. Vincent Island was estimated to be ~1 cm.

The methods used to detect the signal of hurricane deposition in coastal ponds on St. Vincent Island examined cores for evidence of washover sand, marine microfossils, and geochemical data (C and N). Because the proxy records showed marginal evidence of event beds that matched depths with ^{210}Pb ages of known hurricanes, L_s was estimated to be 0-3 cm. The complicating fact is that the thickness of a storm layer would need to be measured directly following a hurricane for an accurate estimate of L_s.

Using the above data and a sedimenation rate of ~2 mm/yr, the equation developed by Wheatcroft and Drake (in press) yields a transit time of 0-5 years (L_b > ~1 cm) for a deposit within the surface mixed zone. The fast transit time suggests that an event layer should be preserved, but does not account for dissipation of the event layer due to physical and biologic mixing. Dissipation time (the time required for an event layer to be

completely destroyed) is best calculated by time-series cores (Wheatcroft and Drake in press). Since time series cores are not available for the ponds on St. Vincent Island, the dissipation time for the cores can be estimated based on estimates of biodiffusion coefficients (D_b), as increased biodiffusion (i.e. bioturbation) should lead to a concomitant increase in dispersion. D_b can be calculated from (a) ^{210}Pb activity data or (b) data from previous studies. ^{210}Pb data can yield measurements of D_b of over decades of mixing if sediments are completely homogenized and there is no sedimentation. Under these conditions, the ^{210}Pb data can be modeled as such:

$$\delta A/\delta t = Db\ (\delta^2 A/\delta z^2) - \lambda A \text{ (i.e., no sedimentation)}$$

where A is ^{210}Pb activity (dpm/g), t is time (years), and z is depth (cm). Since the sediments in the coastal ponds on St. Vincent Island show evidence of bedding (in the x-radiographs) and ^{137}Cs data indicate sedimentation, D_b values can be estimated based on the shape of the ^{210}Pb profile but are most likely very large overestimates. Fitting the data yields a maximum mixing coefficient of 2 cm^2/yr. If contributions from sediment accumulation are also accounted for, the mixing coefficient becomes much smaller. Fitting a mixing profile to the ^{210}Pb activity data could only be done for core OP1 because the data for cores FP1 and FP2 were too variable. Wheatcroft and Drake (in press) report D_b ranging from 10 to 100 cm^2/yr for continental margin sediments where sediments are more biologically active and correspond to dissipation times of 3-5 years. Ravichandran et al. (1995) measured dispersion rates of 0.04 to 0.4 cm^2/yr for a Texas estuary. Dispersion rates for the ponds on St. Vincent Island are estimated to be low, between 0.1 and 2 cm^2/yr, due to the ^{210}Pb estimates and because the x-radiographs showed little evidence of biologically mixed sediments. Laminae preserved within the

sediments would have been destroyed if mixing coefficients were >5 cm^2/yr (Jaeger and Nittrouer in press).

There are not enough observations or data presented by Wheatcroft and Drake (in press) to establish a quantitative relationship between D_b and dissipation time. A semi-quantitative relation can be estimated based on the two relationships that are reported in the paper (D_b=10 cm^2/yr, dissipation time=3 years and D_b=100cm^2/yr, dissipation time=1 year). The estimated D_b values for St. Vincent Island (0.1 to 2 cm^2/yr) yield estimated dissipation times ranging from 5 to 10 years. If dispersion rates on St. Vincent Island are very low due to little biologic activity, and therefore dissipation time is slow, then event layers are more likely to pass through the surface mixed layer partially preserved. If an event layer is thin (<1 cm), then a short dissipation time (<5 years) is likely to result in the destruction of the layer. Since dissipation times of less than five years are not likely to exist on St. Vincent Island (would require D_b>10cm^2/yr), most storm beds should be partially preserved. Obviously, if a storm bed is greater than 1 cm thick, some portion of it will be preserved.

Consequently, the ponds on St. Vincent offer a good environment for studying paleocyclones because they offer an environment with low biologic and physical mixing and thus long dissipation times. The sedimentation rates are low compared to other coastal ponds, but moderate compared to other coastal areas studied for hurricane deposits and lead to fairly fast transit through the surface mixed layer. Because these ponds apparently offer an ideal environment for studying paleocyclone deposits, they should preserve a record of the many large historical hurricanes. However, they show only marginal evidence for storm deposits actually existing within the sediments when

using a variety of proxy records. Diagenetic processes mask evidence of storm deposits and prevent recognition of distinct layers. Thus, one should use caution when examining other published data related to paleocyclone activity.

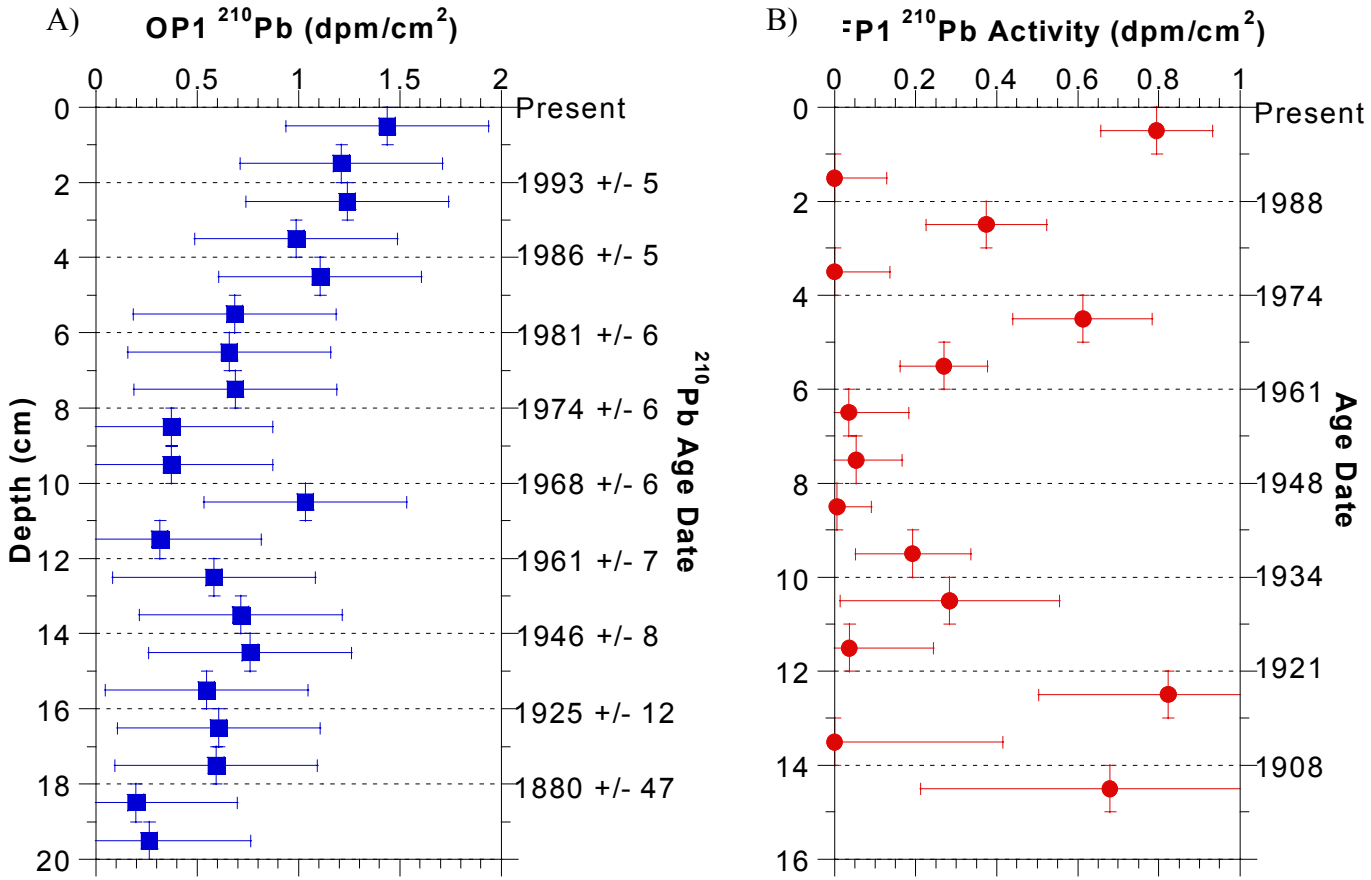

Figure 5-1. ^{210}Pb inventory for cores A) OP1 and B) FP1 calculated by the equation developed by Appleby and Oldfield (1992). Age dates for core OP1 are calculated by the CRS model. Age dates for core FP1 are estimated based on an approximated sediment accumulation rate of 1.5 mm/yr.

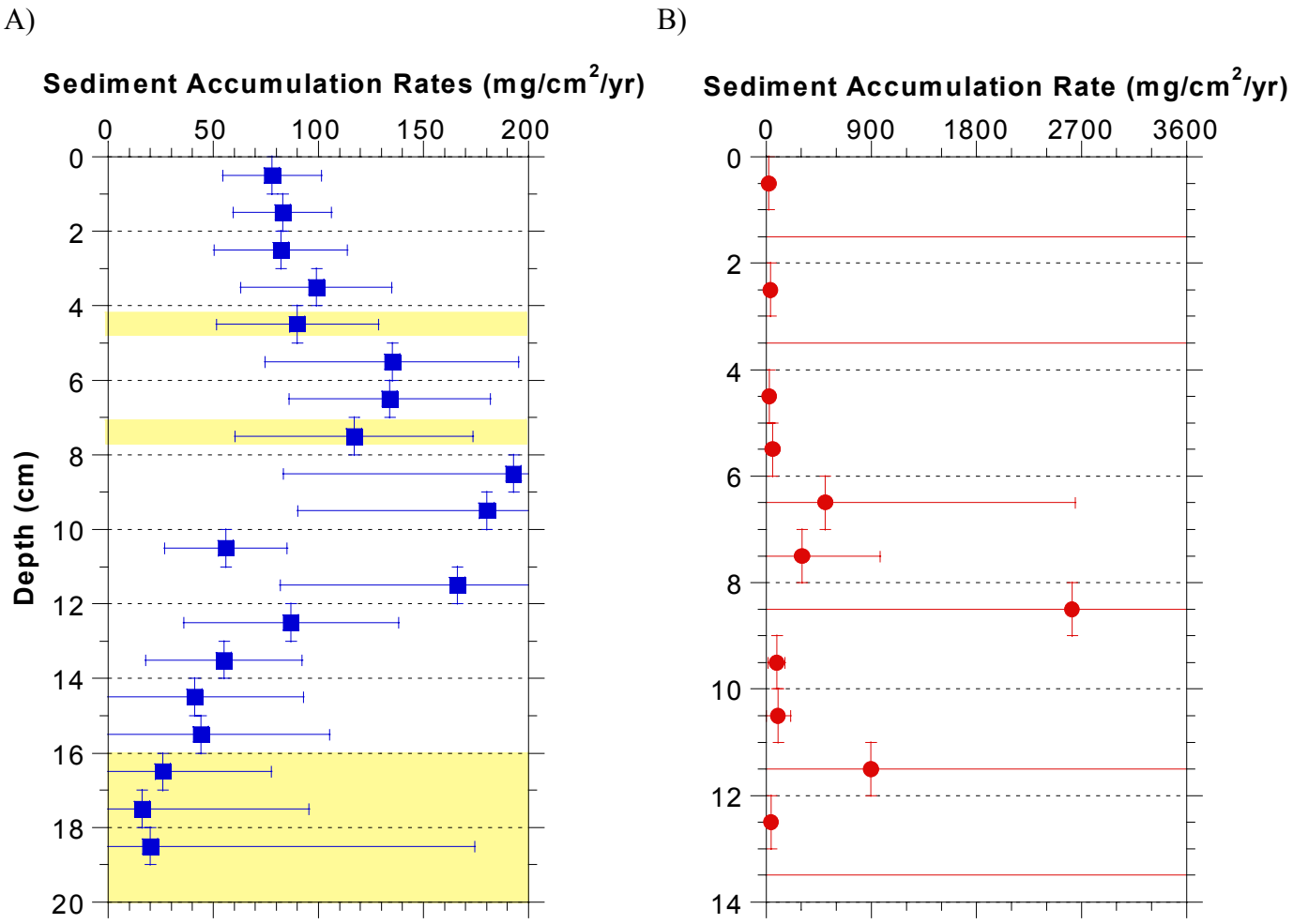

Figure 5-2. Sediment accumulation rates for core A) OP1 and B) FP1 based the CRS model.

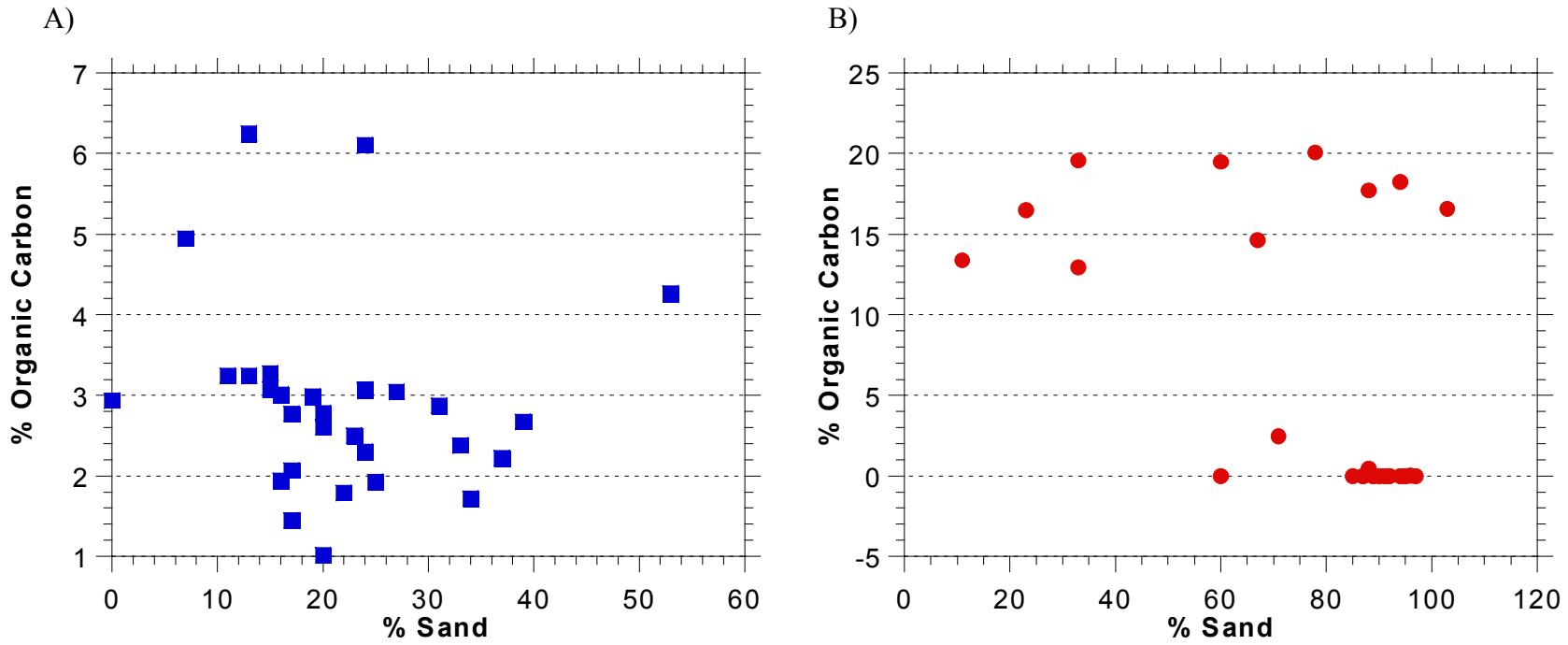

Figure 5-3. Plot of percent sand versus percent organic carbon for cores A) OP1 and B) FP1. Although trends exist in the data, there is no correlation between increased sand and decreased organic carbon. Some core FP1 samples plot above 100% because samples for organic carbon included only a small mass and may not have been representative of the entire sample.

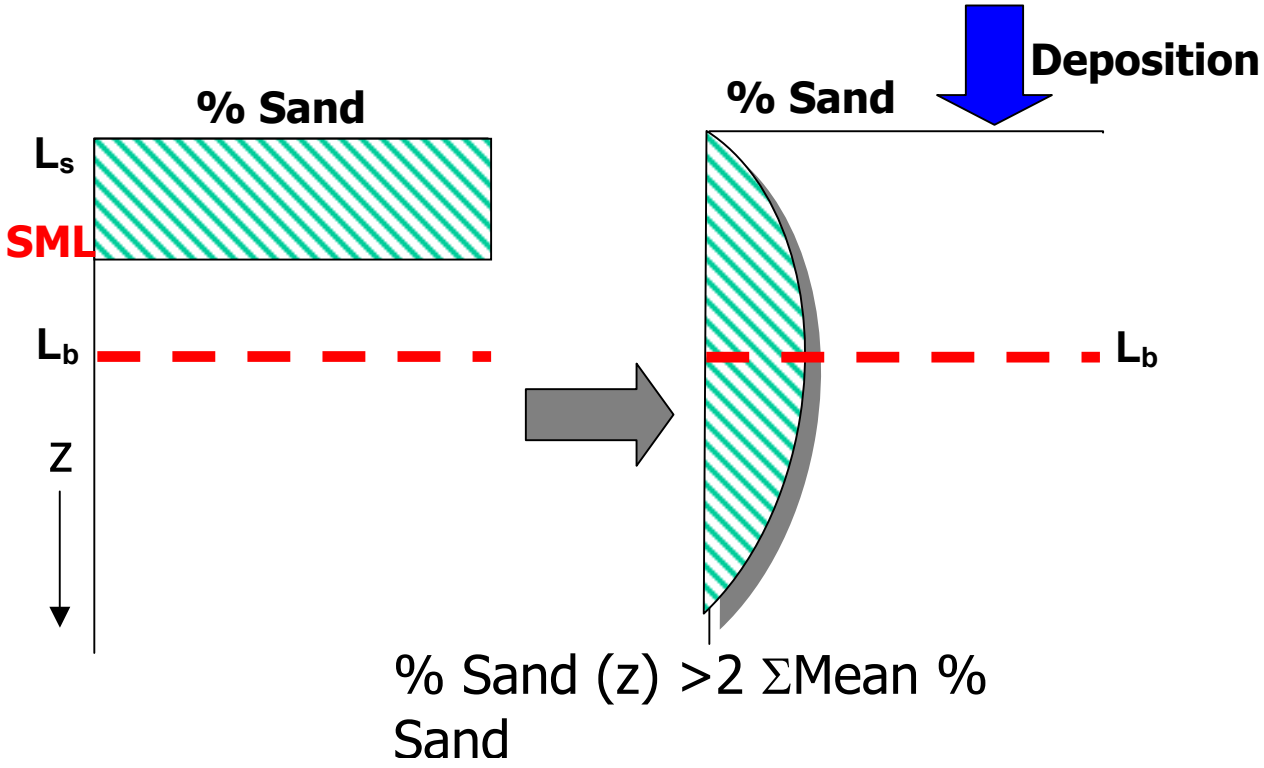

Figure 5-4. Diagram of the preservaton of an event layer after its deposition.

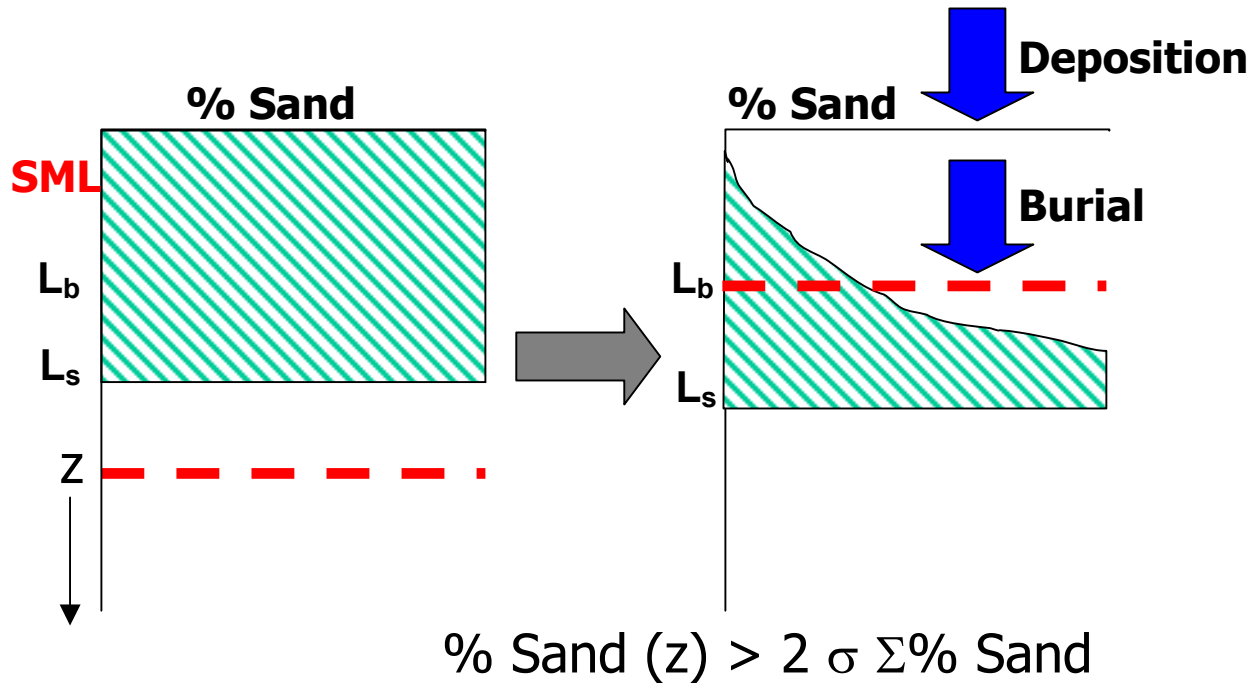

Figure 5-5. Diagram of the destruction of an event layer after its deposition.

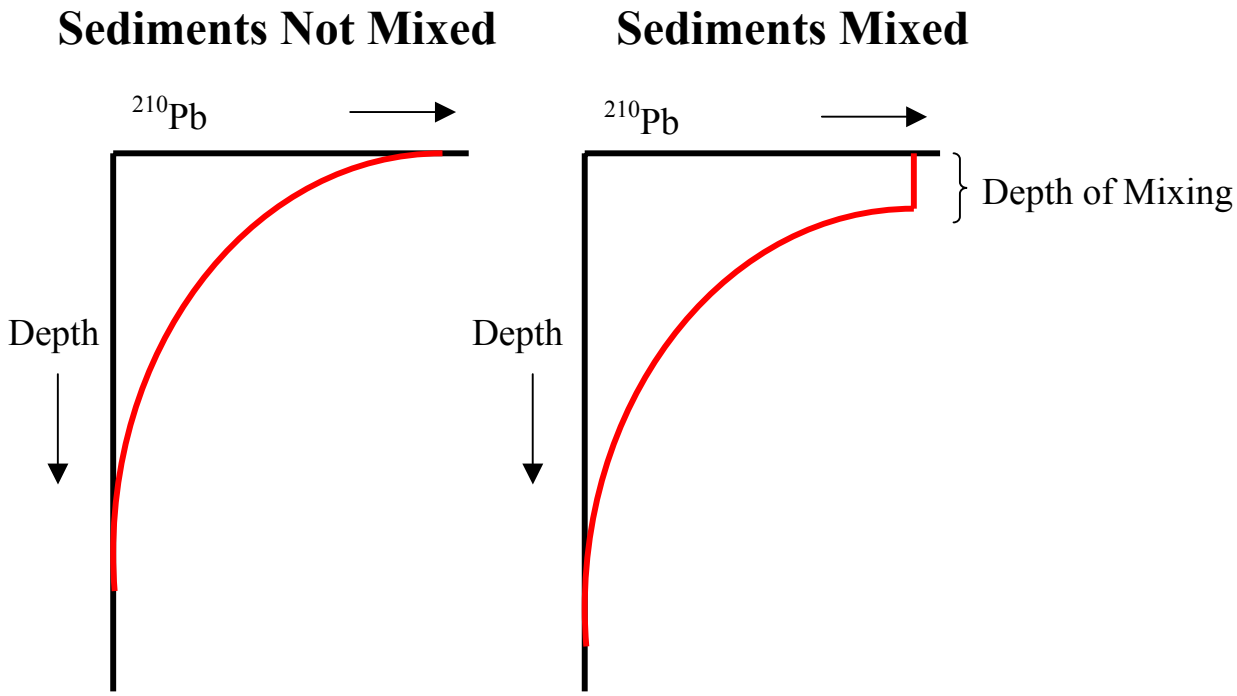

Figure 5-6. Diagram of using ^{210}Pb concentrations to determine the depth of the mixing layer.

CHAPTER 6
CONCLUSION

Establishing a robust age-depth relationship in coastal ponds is difficult because of non-steady, heterogeneous sedimentary conditions. The cores from Flag Pond showed irregular patterns of ^{210}Pb activity due to the high sand content in certain layers of sediment. Ideal coring locations have organic rich sediments that are rich in ^{210}Pb throughout the core.

The results of the preservation potential modeling show that detection of storm bedding is sensitive to sampling interval (1mm vs. 1cm) and coring artifacts (tilted bedding). Depending on storm intensity, event beds may be on the millimeter scale and, therefore, homogenized with non-event bedding during sampling. Also, the cores are placed on their side for splitting which would cause the beds to artificially tilt in the x-radiographs.

The signal left in sediments by hurricane activity is best observed in the x-radiographs, the pixel density data, and percent sand. The x-radiographs and the gray scale pixel intensity data give the highest resolution and can detect sub-centimeter scale event beds. All other proxies require larger sampling intervals in order to have the amount of sample required by the different detection devices. Percent sand showed a possible correlation to the known hurricanes in core OP1, although it was offset from the depth associated with the age of these hurricanes. This proxy is commonly used in paleohurricane studies. A smaller sampling interval would provide more precise data on these deposits because it is likely that storm deposits were partially mixed within the 1

cm sampling interval. Also, constant aeolian transport of sand makes it difficult to distinguish extreme storm event.

The data show very little evidence of storm bedding associated with the three largest storms of the past century (1886, 1974-75, 1985) for the Oyster Pond cores (Table 5-6). Because there is possible evidence of these hurricanes in the percent sand and gray scale intensity data, the L_s for these storms must have been >1 cm. Proxy records that can be recorded while the core is still intact give a better record. It is too difficult to sample a core at intervals less than one centimeter. For proxy records that require the core to be cut into sections, only storms that had an initial L_s of >1 cm will be detected. Data from Flag Pond are overshadowed by the dynamics in sedimentary processes.

Detecting paleocyclone "signal" from natural "noise" of dynamic coastal sedimentary processes is difficult in this location unless signal is very strong. Examples of "noise" on the island are the higher natural sand content and the change in environmental conditions marked by a gradual shift from predominantly organic rich sediments to sand rich sediments.

This research is part of a larger Florida coastal depositional study examining the preservation potential of storm event layers. Additional work will be performed on St. Vincent to better quantify L_b in these ponds and to examine additional sedimentary environments (e.g., salt marshes).

REFERENCES CITED

Appelboom, T.W., Chescheir, G.M., Skaggs, R.W., and Hesterberg, H.L. (2002) Management practices for sediment reduction from forest roads in the coastal plain. *Transactions of the American Society of Agricultural Engineers*, **45** (5), 337-344.

Appleby, P.G. and Oldfield, F. (1992) Application of lead-210 to sedimentation studies. In: *Uranium-series Disequalibrium: Applications to Earth, Marine, and Environmental Sciences, Vol. 0* (Ed. By I.M. and R.S. Harmon), pp. 731-778. Clarendon Press, Oxford.

Ball, M.M., Shinn, E.A. and Stockman, K.W. (1967) Geologic Effects of Hurricane Donna in South Florida. *Journal of Geology*, **75** (5), 583 -587.

Bard, E., Hamelin, B., Arnold, M., Montaggioni, L., Cabioch, G., Faure, G., and Rougerie, F.(1996) Deglacial sea-level record from Tahiti corals and the timing of global meltwater discharge. *Nature*, **382**, 241-244.

Binford, M.W. (1990) Calculations and uncertainty of ^{210}Pb dates for PIRLA project sediment cores. *Journal of Paleolimnology*, **3**, 253-267.

Boudreau, B.P. (1994) Is burial velocity a master parameter for bioturbation? *Geochimica et Cosmochimica Acta*, **58**, 1243-1249.

Brooks, H.K. (1981) Map of Florida. Cooperative Extension Service, University of Florida, Institute for Food and Agricultural Science.

Campbell, K.M. (1986) St. Vincent Island (St. Vincent National Wildlife Refuge), Florida. *Geological Society of America Centennial Field Guide-Southeastern Section*, 351-353.

Collins, E.S., Scott, D.B. and Gayes, P.T. (1999) Hurricane records on the South Carolina coast: Can they be detected in the sediment record? *Quaternary International*, **56**, 15-26.

Committee on Engineering Implications of Changes in Relative Mean Sea Level (1987) *Responding to Changes in Sea Level*. National Academy Press, Washington, D.C., 148 pp.

Davis, J.H. and Mokray, M.F. (2000) Assessment of the effect of road construction and other modifications on surface-water flow at St. Vincent National Wildlife Refuge, Franklin County, Florida. *USGS Water-Resources Investigations Report 00-4007*.

Davis, R.A. (1995) Geologic imapact of Hurricane Andrew on Everglades coast of Southwest Florida. *Environmental Geology*, **25** (3), 143-148.

Davis, R.A., Knowles, S.C. and Bland, M.J. (1989) Role of Hurricanes in the Holocene Stratigraphy of Estuaries – Examples From the Gulf Coast of Florida. *Journal of Sedimentary Petrology*, **59** (6), 1052-1061.

Donnelly, J.P., Bryand, S.S., Butler, J., Dowling, J., Fan, L., Hausmann, N., Newby, P., Shuman, B., Stern, J., Westover, K., and Webb III, T. (2001a) 700 year sedimentary record of intense hurricane landfalls in southern New England. *Geological Society of America Bulletin*, **113** (6), 714-727.

Donnelly, J.P., Roll, S., Wengren, M., Butler, J., Lederer, R., and Webb III, T. (2001b) Sedimentary evidence of intense hurricane strikes from New Jersey. *Geology*, **29** (7), 615-618.

Doyle, T.W. and Krauss, K.W. (1999) The sands and sambars of St. Vincent Island. *Florida Wildlife*, **53** (4), 22-25.

Fisher, M.M., Brenner, M., and Reddy, K.R. (1992) A simple, inexpensive piston corer for collecting undisturbed sediment / water interface profiles. *Journal of Paleolimnology*, **7**, 157-161.

Frederichs, T., Bleil, U., Daumler, K., von Dobeneck, T., and Schmidt, A.M. (1999) The magnetic view on the marine paleoenvironment: parameters, techniques and potentials of rock magnetic studies as a key to paleoclimate and paleoceanographic changes. In: *Use of Proxies in Paleoceanography: Examples from the South Atlantic*, eds. G. Fischer and G. Wefer. Springer-Verlag Berlin Heidelberg, p. 575-599.

Green M.A. and Aller, R.C. (2001) Early diagenesis of calcium carbonate in Long Island Sound sediments: Benthic fluxes of Ca2+ and minor elements during seasonal periods of net dissolution. *Journal of Marine Research*, **59** (5), 769-794.

Hayes, M.O. (1967) Hurricanes as geological agents: Case studies of Hurricane Carla, 1961 and Cindy, 1963. *Rept. Invest. Texas Bur. Econ. Geol., Austin*, **61**, 56 pp.

Ho, F.P. and Myers, V.A. (1975) Joint probability method of tide frequency analysis applied to Apalachicola Bay and St. George Sound, Florida. NOAA Technical Report NWS 18, 43pp.

Hodell, D.A., Curtis, J.H., Jones, G.A., Higuera-Gundy, A., Brenner, M., Binford, M.W., and Dorsey, K.T. (1991) Reconstruction of Caribbean climate change over the past 10,500 years. *Nature*, **353**, 790-793.

Jaeger, J.M. andNittrouer, C.A. (1999) Marine record of surge-induced outburst floods from the Bering Glacier, Alaska. *Geology*, **27**, 847-850.

Jaeger, J.M. and Nittrouer, C.A. (2003) The formation of sedimentary lithofacies on the Gulf of Alaska continental shelf. *Continental Shelf Research*, in press.

Liu, K.B. and Fearn, M.L. (1993) Lake-sediment record of late Holocene hurricane activities from coastal Alabama. *Geology*, **21**, 793-796.

Liu, K.B. and Fearn, M.L. (2000) Reconstruction of prehistoric landfall frequencies of catastrophic hurricanes in northwestern Florida from lake sediment records. *Quaternary Research*, **54** (2), 238-245.

Michaels, A., Malmquist, D., Knap, A., and Close, A. (1997) Climate science and insurance risk. *Nature*, **389**, 225-227.

Norton, S.A., Evans, G.C., and Kahl, J.S. (1997) Comparison of Hg and Pb fluxes to hummocks and hollows of ombrotrophic Big Heath and to nearby Sargent Mt. Pond, Maine, USA. *Water, Air, and Soil Pollution*, **100**, 271-286.

O'Sullivan, P.E., Heathwaite, A.L., Appleby, P.G., Brookfield, D., Crick, M.W., Moscrop, C., Mulder, T.B., Vernon, N.J., and Wilmshurst, J.M. (1991) Paleolimnology of Slapton Ley, Devon, UK. *Hydrobiologia*, **214**, 115-124.

Otvos, E.G. (2002) Letter to the Editor: Discussion of "Prehistoric landfall frequencies of catastrophic hurricanes…" (Liu and Fearn, 2000). *Quaternary Research*, **57**, 425-428.

Parsons, M.L. (1998) Salt marsh sedimentary record of the landfall of Hurricane Andrew on the Louisiana coast; diatoms and other paleoindicators. *Journal of Coastal Research*, **14** (3), 939-950.

Patten, P.C. and Dibble, D.S. (1982) Archeologic and geomorphic evidence for the paleohydrologic record of the Pecos River in west Texas. *American Journal of Science*, **282**, 97-121.

Perkins, R.D. and Enos, P. (1968) Hurricane Betsy in Florida-Bahama Area-Geologic Effects and Comparison With Hurricane Donna. *Journal of Geology*, **76** (6), 710-717.

Pielke, R.A. and Landsea, C.W. (1998) Normalized hurricane damages in the United States: 1925-95. *Weather and Forecasting*, **13** (3), 621-631.

Prewitt, C., Weatherunderground.com, 2003, The Weather Underground, Inc., accessed in 268 Williamson Hall, University of Florida, January 10, 2003.

Prothero, D.R. and Schwab, F. (1996) *Sedimentary Geology: An introduction to sedimentary rocks and stratigraphy*. W. H. Freeman and Company, New York. p. 33.

Ravichandran, M., Baskaran, M., Santschi, P.H., and Bianchi, T.S. (1995) Geochronology of sediments in the Sabine-Neches estuary, Texas, U.S.A. *Chemical Geology*, **125**, 291-306.

Risi, J.A. (1998) Event sedimenation from Hurricane Andrew along the Southwes Florida coast, University of Miami, Ph.D. Dissertation, 199 pp.

Rose, P.R. and Lidz, B. (1977) Diagnostic foraminifera assemblages of shallow-water modern environments : South Florida and the Bahamas. Comparative Sedimentology Laboratory, Division of Marine Geology and Geophysic, Rosenstiel School of Marine and Atmospheric Science, The University of Miami, 56p.

Ruiz-Fernandez, A.C., Hillaire-Marcel, C., Ghaleb, B., Paez-Osuna, F., and Soto-Jimenez, M. (2001) Isotopic constraints (^{210}Pb,^{228}Th) on the sedimentary dynamics of contaminated sediments from a subtropical coastal lagoon (NW Mexico). *Environmental Geology*, DOI 10.1007/s002540100341.

St. Vincent National Wildlife Refuge, Apalachicola, Fl. (1968) 1968 Narrative Report. US Department of the Interior, Fish and Wildlife Service, Bureau of Sport Fisheries and Wildlife, 23p.

St. Vincent National Wildlife Refuge, Apalachicola, Fl. (2000a) Wildlife and Habitat Management Review, May 31-June 2, 2000.

St. Vincent National Wildlife Refuge, Apalachicola, Fl. (2000b) Final Report of the Vegetation Survey and Map Project, A USFWS-USGS Research Partnership Program Project.

Santschi, P.H., Li, Y.H., Bell, J.J., Trier, R.M., and Kawtaluk, K. (1980) Pu in coastal marine environment. *Earth Planetary Science Letters*, **39**, 248-265.

Schelske, C.L., Kenney, W.F., and Whitmore, T.J. (2001) Sediment and nutrient deposition in Harris Chain-of-Lakes. *Special Publication SJ2001-SP7*, Department of Fisheries and Aquatic Sciences, University of Florida, Gainesville, Fl.

Schelske, C.L., Peplow, A., Brenner, M., and Spencer, C.N. (1994) Low-background gamma counting: applications for ^{210}Pb dating of sediments. *Journal of Paleolimnology*, **10**, 115-128.

Scott, L. and Steenkamp, M. (1996) Environmental history and recent human influence at coastal Lake Teza, KwaZulu-Natal. *South African Journal of Science*, **92**, 348-350.

Smith, J.T. and Comans, R.N. (1996) Modeling the diffusive transport and remobilization of ^{137}Cs in sediments: The effects of sorption kinetics and reversibility. *Geochimica et Cosmochimica Acta*, **60**, 995-1004.

Sugai, S.F., Alperin, M.J., and Reeburgh, W.S. (1994) Episodic deposition and ^{137}Cs immobility in Skan Bay sediments: A ten-year ^{210}Pb and ^{137}Cs time series. *Marine Geology*, **116**, 351-372.

Syvitski, J.P.M., Asprey, K.W., and Clattenburg, D.A. (1991) Principles, design, and calibration of settling tubes. In: *Principles, Methods, and Application of Particle Size Analysis*, ed. Syvitski, J.P.M. Cambridge, U.K.: Cambridge University Press, pp. 45-63.

Turekian, K.K., Nozaki, Y., and Benninger, L. (1977) Geochemistry of atmospheric radon and radon products. *Earth and Planetary Sciences Annual Review*, **5**, 1018-1021.

Weber, M.E., Niessen, F. Kuhn, G., and Wiedicke, M. (1997) Calibration and application of marine sedimentary physical properties using a multi-sensor core logger. *Marine Geology*, **136**, 151-172.

Wheatcroft, R.A. and Drake, D.E. (2002) Post-depositional alteration and preservation of sedimentary event layers on continental margins, I. The role of episodic sedimentation. Submitted to *Marine Geology*, 10 May 2002.

Wheeler, A.J., Oldfield, F., and Orford, J.D. (1999) Depositional and post-depositional magnetic signals from saltmarshes on the north-west coast of Ireland. *Sedimentology*, **46**(3), 545-556.

Williams, F.L. (1995) Foraminiferal record of recent environmental change: Mad Island Lake, Texas. *Journal of Foraminiferal Research*, **25** (2), 167-179.

Williams, J.M. and Duedell, I.W. (1997) *Florida Hurricanes and Tropical Storms.* Gainesville: University of Press of Florida, 146 pp.

BIOGRAPHICAL SKETCH

Marylea Hart was born in Greenville, SC on December 29, 1977. She moved to Georgetown, SC at the age of two and then to Columbia, SC at the age of nine. She graduated from Richland Northeast High School in 1996. Marylea earned a Bachelor of Science degree in geology from Furman University in 2000. She then moved on to the University of Florida to study for a Master of Science degree in geology. She is currently employed by Geohazards, Inc. in Gainesville, FL.